

© 2017 Naga Saras Chandan Vempati

INVESTIGATION ON WEAKLY CURVED COUNTERFLOW
DIFFUSION FLAMES AT INFINITELY FAST CHEMISTRY

BY

NAGA SARAS CHANDAN VEMPATI

THESIS

Submitted in partial fulfillment of the requirements
for the degree of Master of Science in Mechanical Engineering
in the Graduate College of the
University of Illinois at Urbana-Champaign, 2017

Urbana, Illinois

Adviser:

Professor Moshe Matalon

ABSTRACT

We investigate the behavior of a counterflow diffusion flame subject to a flow field comprising of a first order potential flow superimposed on a weak second order correction to the potential flow. An Arrhenius one-step irreversible reaction model at infinite Damköhler number and constant density is considered. This simplified model is then used to study the distribution of fuel and oxidizer mass fractions, shape of the reaction sheet, and the temperature field. The temperature of the reaction sheet for the unity Lewis numbers is constant and is shown to be equal to the adiabatic flame temperature. The temperature of the reaction for the unequal Lewis number case is also shown to be constant and is equal to the stoichiometric flame temperature. In addition, we also show that the reaction sheet always takes the shape of the separatrix, independent of fuel-oxidizers Lewis numbers and mixture strength.

To the next person working on this

ACKNOWLEDGEMENTS

I would like to express my gratitude to my advisers, Prof. Moshe Matalon and Prof. Carlos Pantano for giving me the opportunity to work on this problem. Their deep physical insight and dedication to research was inspirational.

I would also like to take this opportunity to thank Ms. Jennifer Carlson of Department of Electrical and Computer Engineering, and Ms. Kathryn Smith of the Department of Mechanical Science and Engineering for hiring me as a Teaching Assistant without which I wouldn't have been able to work on my Master's thesis here at UIUC. I also had the privilege of meeting exceptional students such as Sandeep, Raja. Their support was valuable to get me through tough times.

Lastly, I would like to express my sincere gratitude to my parents, brother, grandmothers, and Naperville Bhagis without whose encouragement and emotional support I wouldn't have made it this far.

TABLE OF CONTENTS

LIST OF FIGURES	vii
LIST OF TABLES	ix
LIST OF SYMBOLS	x
CHAPTER 1 INTRODUCTION	1
CHAPTER 2 MATHEMATICAL DESCRIPTION AND GOV- ERNING EQUATIONS	4
2.1 Boundary Conditions	9
CHAPTER 3 WEAKLY CURVED FLAMES	10
3.1 Flow Field	10
CHAPTER 4 UNITY LEWIS NUMBERS CASE	12
4.1 Temperature Distribution for Unity Lewis Numbers	18
CHAPTER 5 UNEQUAL LEWIS NUMBERS CASE	20
CHAPTER 6 TEMPERATURE DISTRIBUTION IN UNEQUAL LEWIS NUMBER CASE	27
CHAPTER 7 RESULTS	32
7.1 Unity Lewis Numbers Case	32
7.2 Unequal Lewis Numbers Case	39
CHAPTER 8 CONCLUSIONS	46
REFERENCES	48
APPENDIX A NUMERICAL METHODOLOGY TO SOLVE THE $\mathcal{O}(\epsilon)$ EQUATION FOR Z	49
APPENDIX B NUMERICAL METHODOLOGY TO SOLVE FOR $\mathcal{O}(\epsilon)$ COMPONENT OF \hat{Z}	53

APPENDIX C	NUMERICAL METHODOLOGY TO SOLVE FOR	
$T^{(1)}$	54
C.1	Numerical Methodology	54
C.2	Immersed Interface Method	56

LIST OF FIGURES

1.1	Combustion System	3
3.1	Flow Fields for different α	11
4.1	Comparison of Positions of Reaction Sheet using various approaches for $\phi = 1$	18
7.1	Variation of $\hat{Z}^{(0)}$ for $\mathcal{L}_F=1, \mathcal{L}_O=1$ and $\phi=0.5$	33
7.2	Variation of $\hat{Z}^{(1)}$ for $\mathcal{L}_F=1, \mathcal{L}_O=1$ and $\phi=0.5$	33
7.3	Variation of $T^{(0)}$ for $\mathcal{L}_F=1, \mathcal{L}_O=1$ and $\phi=0.5$	34
7.4	Variation of $T^{(1)}$ for $\mathcal{L}_F=1, \mathcal{L}_O=1$ and $\phi=0.5$	34
7.5	Variation of $\hat{Z}^{(0)}$ for $\mathcal{L}_F=1, \mathcal{L}_O=1$ and $\phi=1$	35
7.6	Variation of $\hat{Z}^{(1)}$ for $\mathcal{L}_F=1, \mathcal{L}_O=1$ and $\phi=1$	35
7.7	Variation of $T^{(0)}$ for $\mathcal{L}_F=1, \mathcal{L}_O=1$ and $\phi=1$	36
7.8	Variation of $T^{(1)}$ for $\mathcal{L}_F=1, \mathcal{L}_O=1$ and $\phi=1$	36
7.9	Variation of $\hat{Z}^{(0)}$ for $\mathcal{L}_F=1, \mathcal{L}_O=1$ and $\phi=2$	37
7.10	Variation of $\hat{Z}^{(1)}$ for $\mathcal{L}_F=1, \mathcal{L}_O=1$ and $\phi=2$	37
7.11	Variation of $T^{(0)}$ for $\mathcal{L}_F=1, \mathcal{L}_O=1$ and $\phi=2$	38
7.12	Variation of $T^{(1)}$ for $\mathcal{L}_F=1, \mathcal{L}_O=1$ and $\phi=2$	38
7.13	Variation of $\hat{Z}^{(0)}$ for $\mathcal{L}_F=1.5, \mathcal{L}_O=1.5$ and $\phi=0.5$	40
7.14	Variation of $\hat{Z}^{(1)}$ for $\mathcal{L}_F=1.5, \mathcal{L}_O=1.5$ and $\phi=0.5$	40
7.15	Variation of $T^{(0)}$ for $\mathcal{L}_F=1.5, \mathcal{L}_O=1.5$ and $\phi=0.5$	41
7.16	Variation of $T^{(1)}$ for $\mathcal{L}_F=1.5, \mathcal{L}_O=1.5$ and $\phi=0.5$	41
7.17	Variation of $\hat{Z}^{(0)}$ for $\mathcal{L}_F=1.5, \mathcal{L}_O=1.5$ and $\phi=1$	42
7.18	Variation of $\hat{Z}^{(1)}$ for $\mathcal{L}_F=1.5, \mathcal{L}_O=1.5$ and $\phi=1$	42
7.19	Variation of $T^{(0)}$ for $\mathcal{L}_F=1.5, \mathcal{L}_O=1.5$ and $\phi=1$	43
7.20	Variation of $T^{(1)}$ for $\mathcal{L}_F=1.5, \mathcal{L}_O=1.5$ and $\phi=1$	43
7.21	Variation of $\hat{Z}^{(0)}$ for $\mathcal{L}_F=1.5, \mathcal{L}_O=1.5$ and $\phi=2$	44
7.22	Variation of $\hat{Z}^{(1)}$ for $\mathcal{L}_F=1.5, \mathcal{L}_O=1.5$ and $\phi=2$	44
7.23	Variation of $T^{(0)}$ for $\mathcal{L}_F=1.5, \mathcal{L}_O=1.5$ and $\phi=2$	45
7.24	Variation of $T^{(1)}$ for $\mathcal{L}_F=1.5, \mathcal{L}_O=1.5$ and $\phi=2$	45
A.1	Sample Computational Domain	50
A.2	Results of Grid Dependency Studies	52
C.1	Arrangement of the grid points about the position $x_f^{(0)}$	54

C.2 Results of Grid Dependency studies on $T^{(1)}$ in terms of the L^1 norm, $\|T^{(1)}\|_1$ for $\mathcal{L}_F = 1.5$, $\mathcal{L}_O = 0.5$ and $\phi = 1$ as a function of the number of grid points, N 62

LIST OF TABLES

7.1	Combinations of physical parameters considered for the unequal Lewis numbers case	32
7.2	Combinations of physical parameters considered for the unequal Lewis numbers case	39

LIST OF SYMBOLS

Greek symbols

α	Factor measuring the strength of 2^{nd} degree potential flow field
β	Activation-energy parameter
$\Delta\eta$	Grid size along η direction
Δx	Grid size along x -direction
$\delta(x)$	Dirac-delta distribution
ϵ	Small parameter
η	Scaled y-axis
$\bar{\phi}$	Potential function
Φ	Modified initial mixture strength
ϕ	Initial mixture strength
γ	Strain rate
χ	$\mathcal{O}(\epsilon)$ component of x_f
χ'	Partial derivative of χ with respect to x
λ	Thermal conductivity
μ	Coefficient of viscosity
ν_F	Stoichiometric coefficient of Fuel
ν_O	Stoichiometric coefficient of Oxidizer

$\tilde{\nabla}$	Gradient operator
∇	Non-dimensional gradient operator
$\tilde{\omega}$	Rate of reaction
ω	Non-dimensional rate of reaction
$\tilde{\rho}$	Density
$\tilde{\rho}_0$	Charateristic density
ρ	Non-dimensional density
ψ	Stream function
Σ	Summation
τ	Truncation error
$\theta(k)$	Correction function

Latin symbols

\mathcal{B}	Pre-exponential factor
c_p	Specific heat at constant pressure
\mathcal{D}_{th}	Thermal Diffusivity
\mathcal{D}_i	Molecular diffusivity of species i
D	Damköhler number
erf^{-1}	Inverse error function
E	Activation Energy
$\text{erf}(x)$	Error function
$\text{erfc}(x)$	Complimentary error function
F	Fuel
\bar{H}	Heaviside function

H_n	Hermite polynomial of degree n
I	Grid point corresponding to $x = x_f^{(0)}$
\mathcal{L}	Lewis number distribution
$\mathcal{L}_{\mathcal{F}}$	Lewis Number of Fuel
$\mathcal{L}_{\mathcal{O}}$	Lewis Number of Oxidizer
\mathcal{L}_i	Lewis number of species i
L	Length of the domain
L^1	L^1 norm
W	Height of the domain
M	Number of grid points in the η -direction
N	Number of grid points in the x -direction
n	Position vector of the outward normal
\mathcal{O}	Big Oh
O	Oxidizer
\tilde{p}	Pressure
\tilde{P}_c	Constant ambient pressure
Pr	Prandtl number
p	Non-dimensional pressure
Q	Amount of heat released
q	Heat release parameter
R	Universal Gas constant
st	Stoichiometric
$\tilde{T}_{-\infty}$	Temperature at inlets

\tilde{T}	Temperature
\tilde{t}	Time
T_a	Adiabatic temperature
T_s	Stoichiometric temperature
T	Non-dimensional temperature
t	Non-dimensional time
\tilde{u}	Velocity in x-direction
u	Non-dimensional velocity along x-axis
\tilde{V}	Velocity Field
\tilde{v}	Velocity in y-direction
V	Non-dimensional velocity vector
v	Non-dimensional velocity along y-axis
V_1	Second order potential flow field
\overline{W}	Mixture molecular weight
W_i	Molecular weight of species i
$X^{(0)}$	$\mathcal{O}(1)$ component of some quantity X
$X^{(1)}$	$\mathcal{O}(\epsilon)$ component of some quantity X
x_f	Position of reaction sheet
\tilde{Y}_{F_u}	Fuel mass fraction at inlet
\tilde{Y}_F	Fuel mass fraction
\tilde{Y}_{O_u}	Oxidizer mass fraction at inlet
\tilde{Y}_O	Oxidizer mass fraction
Y_F	Non-dimensional fuel mass fraction

Y_O	Non-dimensional oxidizer mass fraction
\widetilde{Y}_F	Molecular weight of fuel
\widetilde{Y}_O	Molecular weight of oxidizer
\hat{Z}	Modified mixture fraction
\hat{Z}_{st}	Stoichiometric modified mixture fraction
Z	Mixture fraction
Z_{1N}	Numerical solution of $Z^{(1)}$ corresponding to N grid points in x and η direction
Z_{1ref}	Analytical solution of $Z^{(1)}$
Z_{st}	Stoichiometric mixture fraction

Other Symbols and abbreviations

$D/D\tilde{t}$	Total derivative
D/Dt	Non-dimensional total derivative
IIM	Immersed Interface Method
LHS	Left hand side
ODE	Ordinary differential equation
PDE	Partial differential equation
RHS	Right hand side

CHAPTER 1

INTRODUCTION

Combustion, without any stretch of hyperbole, is the most important reaction known to man. It is also one of the most complex physical phenomenon known. The governing equations of combustion or chemically reacting flows, the Navier-Stokes equations supplemented by the mass balance of species involved in combustion are difficult to solve numerically and probably impossible to solve analytically. Thus, the treatment of these equations require simplifications based on physical reasoning. Fundamental understanding of the physics of a combustion system is best achieved by making these simplifications. The models built based on these simplifications retain the main features of combustion and the simplified governing equations thus obtained can be solved analytically or numerically to gain rich insight into the physical phenomena occurring at various regions of flow field and their effects on the system as a whole.

In general, flames are divided into types: Premixed flames in which the fuel and oxidizer are premixed before ignition occurs, and diffusion flames where fuel and oxidizer meet coinciding with the onset of combustion. In this document, we will concern ourselves with diffusion flames.

In diffusion flames, the reaction between occurs at the interface between the fuel and oxidizer. Further, the rate of burning depends more upon the rate of mixing than on the rates of the chemical processes involved. Some of the types of diffusion flames are combustion of a spherical fuel droplet, jet diffusion flames etcetera. But, the most commonly studied type of diffusion flame is the counterflow diffusion flame. In the classical problem of a counterflow diffusion flame, a stream of gas containing fuel, usually mixed with a noble gas emanating at one end impinges against another stream of gas containing the oxidizer emanating at the opposite end as shown in the

Figure (1.1). It is assumed that at the far left of the system there is only fuel and no oxidizer and vice-versa on the far right. The reaction takes place in a region called the reaction zone.

Theories of diffusion flames find their roots in the seminal work by Burke and Schumann (1928). This paper provides a mathematical description for diffusion flames by introducing the infinite rate chemistry limit or the Burke-Schumann limit. Their paper also hypothesized that the fuel and oxidizer arriving from opposing ends are instantaneously and completely consumed along the interface where they meet. It was realized in subsequent works [Kassoy and Williams (1968)] that the Burke-Schumann limit corresponds to the asymptotic limit of large Damköhler number, D , which represents the ratio of flow time to the chemical reaction time. Further, it was found that the interface where the fuel and oxidizer meet is a thin reactive-diffusive layer of thickness of the order, $D^{-1/3}$. This thin layer is called the *Reaction Sheet*. This reaction sheet divides the combustion system into two regions: the fuel region, where there is no oxidizer, and the oxidizer region where there is no fuel. The fuel and oxidizer regions are reaction free and are dominated by convective-diffusive transport and all the chemical activity is confined to the reaction sheet.

One of the aspects of counterflow diffusion flames that has not been investigated yet is how the reaction sheet behaves when it is curved. Thus, the objective of this article is to investigate the shape and temperature of the reaction sheet at the Burke-Schumann limit and hence further our understanding of counterflow diffusion flames. We divide our investigation into two parts- the first being the case when the Lewis numbers of the fuel and oxidizer are unity, and the second when the Lewis numbers of the fuel and oxidizers are unequal. To achieve our objective, we build a lower order model of the combustion system instead of solving the entire gamut of the governing equations. The details of this model are given in the subsequent chapters.

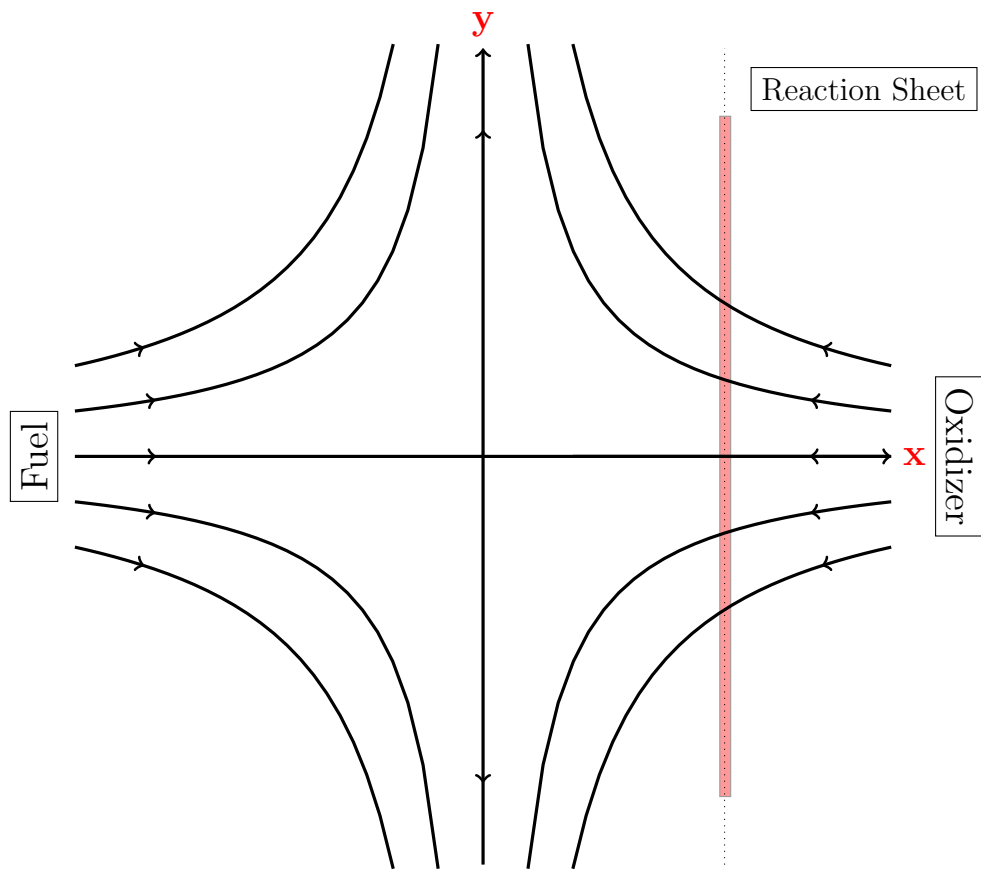


Figure 1.1: Combustion System

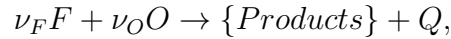
CHAPTER 2

MATHEMATICAL DESCRIPTION AND GOVERNING EQUATIONS

In a classical counterflow diffusion flame, as given in figure (1.1) of the previous chapter, the velocity field, \tilde{V} as a function of coordinates (x, y) is given by,

$$\tilde{V}(x, y) = (\tilde{u}, \tilde{v}) = (-2\gamma x, 2\gamma y), \quad (2.1)$$

where γ is the strain rate (with units 1/s). Further, in our problem, the chemical activity is modeled according to the one step irreversible reaction,



where F and O identify the fuel and oxidizer respectively, ν_F and ν_O are the stoichiometric coefficients corresponding to fuel and oxidizer respectively, and Q is the total heat release in the process. The equation is assumed to be the Arrhenius type with overall activation energy E and pre-exponential factor, \mathcal{B} . Assuming first order dependence of the rate of reaction on both the fuel and oxidizer, the reaction rate is of the form,

$$\tilde{\omega} = \mathcal{B} \left(\frac{\tilde{\rho} \tilde{Y}_F}{W_F} \right) \left(\frac{\tilde{\rho} \tilde{Y}_O}{W_O} \right) e^{-E/R\tilde{T}},$$

where $\tilde{\rho}$, \tilde{T} are the density and temperature of the mixture, W_i the molecular weight of species i ; R is the universal gas constant. The tilde denotes dimensional quantities. Let \tilde{p} be the pressure, \tilde{Y}_F and \tilde{Y}_O the fuel and oxidizer mass fractions, the governing equations of the system assuming no body

forces are:

$$\frac{\partial \tilde{\rho}}{\partial t} + \tilde{\nabla} \cdot \tilde{\rho} \tilde{V} = 0, \quad (2.2)$$

$$\tilde{\rho} \frac{D\tilde{V}}{Dt} = -\tilde{\nabla} \tilde{p} + \mu \tilde{\nabla}^2 \tilde{V}, \quad (2.3)$$

$$\tilde{\rho} c_p \frac{D\tilde{T}}{Dt} - \tilde{\nabla} \cdot (\lambda \tilde{\nabla} \tilde{T}) = Q \tilde{\omega}, \quad (2.4)$$

$$\tilde{\rho} \frac{D\tilde{Y}_F}{Dt} - \tilde{\nabla} \cdot (\tilde{\rho} \mathcal{D}_F \tilde{\nabla} \tilde{Y}_F) = -\nu_F W_F \tilde{\omega}, \quad (2.5)$$

$$\tilde{\rho} \frac{D\tilde{Y}_O}{Dt} - \tilde{\nabla} \cdot (\tilde{\rho} \mathcal{D}_O \tilde{\nabla} \tilde{Y}_O) = -\nu_O W_O \tilde{\omega}. \quad (2.6)$$

The above equations represent the mass, momentum, and energy of the whole mixture and species equations for fuel and oxidizer respectively. The operator D/Dt , represents the substantial derivative and ∇ , the gradient operator. The mixture properties are identified as thermal conductivity, λ ; specific heat at constant pressure, c_p ; coefficient of viscosity (μ). These properties are assumed to be constant with respect to the thermodynamic quantities. Further, the molecular diffusivities are assumed to be linearly dependent on temperature such that $\rho \mathcal{D}_i$ are independent of temperature. The reaction is assumed to be taking place in open space with the characteristic velocity much less than the speed of sound because of which it can be assumed that the changes in pressure due to change in momentum as governed by equation (2.3) are negligible. Under this assumption, the pressure of the combustion system, \tilde{P} can be assumed to be equal to constant, say \tilde{P}_c . Subsequently, the equation of state boils down to

$$\tilde{P}_c = \tilde{\rho} R \tilde{T} / \bar{W}, \quad (2.7)$$

where \bar{W} is the molecular weight of the mixture which is also assumed to be constant. Equations (2.2)-(2.7) are non-dimensionalized as follows:

The mass fractions of the fuel and oxidizer at their corresponding inlets are \tilde{Y}_{F_u} and \tilde{Y}_{O_u} respectively. The local mass fractions of the fuel and oxidizer are normalized with \tilde{Y}_{F_u} and \tilde{Y}_{O_u} respectively and we thus obtain,

$$Y_F = \frac{\tilde{Y}_F}{\tilde{Y}_{F_u}},$$

$$Y_O = \frac{\tilde{Y}_O}{\tilde{Y}_{O_u}}.$$

Length, velocity and time are scaled with respect to $(\mathcal{D}_{th}/\gamma)^{1/2}$, $(\mathcal{D}_{th}\gamma)^{1/2}$ and $1/\gamma$ respectively, where γ is the characteristic strain rate, $\mathcal{D}_{th} = \lambda/\tilde{\rho}_0 c_p$ is the thermal diffusivity where $\tilde{\rho}_0$ is the characteristic density. Pressure is scaled with $\tilde{P}_0 = \lambda\gamma/c_p$; temperature is scaled with $\tilde{T}_{-\infty}$, which is the temperature at the fuel and oxidizer inlets. Density is scaled with $\tilde{\rho}_0 = \lambda\gamma\bar{W}/c_p R\tilde{T}_{-\infty}$. The rate of reaction $\tilde{\omega}$ is scaled with $\tilde{\omega}_0 = \tilde{\rho}_0\tilde{Y}_{F_u}\gamma/\nu_F W_F$. After non-dimensionalizing, the following set of equations are obtained:

$$\frac{\partial \rho}{\partial t} + \nabla \cdot \rho V = 0, \quad (2.8)$$

$$\rho \frac{DV}{Dt} = -\nabla p + Pr \nabla^2 V, \quad (2.9)$$

$$\rho \frac{DT}{Dt} - \nabla^2 T = q\omega, \quad (2.10)$$

$$\rho \frac{DY_F}{Dt} - \frac{1}{\mathcal{L}_F} \nabla^2 Y_F = -\omega, \quad (2.11)$$

$$\rho \frac{DY_O}{Dt} - \frac{1}{\mathcal{L}_O} \nabla^2 Y_O = -\phi\omega, \quad (2.12)$$

$$\omega = D\rho^2 Y_F Y_O \exp \left\{ \frac{\beta(T - T_a)}{TT_a} \right\}. \quad (2.13)$$

In equation (2.13), ω is the non-dimensionalized chemical reaction rate; T_a is the non-dimensionalized adiabatic temperature. Other parameters in these equations are: Lewis numbers $\mathcal{L}_F = \mathcal{D}_{th}/\mathcal{D}_F$ of the fuel and $\mathcal{L}_O = \mathcal{D}_{th}/\mathcal{D}_O$ of the oxidizer; the heat release parameter $q = Q\tilde{Y}_{F_u}/\nu_F W_F c_p \tilde{T}_{-\infty}$; the activation-energy parameter $\beta = E/R\tilde{T}_{-\infty}$; the Prandtl number $Pr = \mu c_p/\lambda$.

ϕ is called the initial mixture strength which is the ratio of the oxidizer mass fraction supplied to the oxidizer side and the mass fraction of the fuel supplied to the fuel side normalized the mass-averaged stoichiometric coeffi-

cient ratio, ν , hence,

$$\nu = \frac{\nu_O W_O}{\nu_F W_F},$$

$$\phi = \frac{\tilde{Y}_{F_u}/\tilde{Y}_{O_u}}{1/\nu} = \frac{\tilde{Y}_{F_u}/\nu_F W_F}{\tilde{Y}_{O_u}/\nu_O W_O}.$$

The Damköhler number, D , is given by

$$D = \frac{\mathcal{B}\tilde{\rho}_0\tilde{Y}_{O_u}\nu_O W_O}{\gamma} \exp\left(\frac{-\beta}{T_a}\right) \quad (2.14)$$

Because of the non-linear nature of the governing equations, we make certain assumptions in order to make the problem more tractable. Firstly, we assume the reaction to occur at the Burke-Schumann limit— this corresponds to an infinite Damköhler number, i.e, the reaction time is much shorter than the flow time. Under this assumption, all the chemical reactions are confined to the reaction sheet with no chemical activity in the other regions in the domain. Further, to decouple the momentum equation from the energy and species equations, we assume that the density is constant and hence, $\rho = 1$. Invoking the aforementioned assumptions and assuming the system to be at steady state, the governing equations modify into:

$$\frac{\partial u}{\partial x} + \frac{\partial v}{\partial y} = 0, \quad (2.15)$$

$$u \frac{\partial u}{\partial x} + v \frac{\partial u}{\partial y} = -\frac{\partial p}{\partial x}, \quad (2.16)$$

$$u \frac{\partial v}{\partial x} + v \frac{\partial v}{\partial y} = -\frac{\partial p}{\partial y}, \quad (2.17)$$

$$u \frac{\partial T}{\partial x} + v \frac{\partial T}{\partial y} - \nabla^2 T = 0, \quad (2.18)$$

$$u \frac{\partial Y_F}{\partial x} + v \frac{\partial Y_F}{\partial y} - \frac{1}{\mathcal{L}_F} \nabla^2 Y_F = 0, \quad (2.19)$$

$$u \frac{\partial Y_O}{\partial x} + v \frac{\partial Y_O}{\partial y} - \frac{1}{\mathcal{L}_O} \nabla^2 Y_O = 0. \quad (2.20)$$

It has to noted that equation (2.19) is valid in the fuel region and equation (2.20) is valid in the oxidizer region. Because of the assumption of infinite rate chemistry and more importantly because of fact that the chemical activity

is confined to the reaction sheet, the temperature and mass fractions are continuous across the reaction sheet (whose position is given by x_f), but their derivatives aren't and hence we have to supply appropriate jump conditions to close the problem. They are as follows:

$$[[T]]_{x_f} = [[Y_F]]_{x_f} = [[Y_O]]_{x_f} = 0, \quad (2.21)$$

$$\left[\left[\frac{\partial T}{\partial n} \right] \right]_{x_f} = -\frac{q}{\mathcal{L}_F} \left[\left[\frac{\partial Y_F}{\partial n} \right] \right]_{x_f} = -\frac{q}{\phi \mathcal{L}_O} \left[\left[\frac{\partial Y_O}{\partial n} \right] \right]_{x_f}, \quad (2.22)$$

where n is the direction of the local normal of the reaction sheet. Further, $[[\cdot]]_{x_f}$ denotes the jump in the quantity in the brackets across the coordinate given by the subscript, x_f .

Further, in the theoretical treatment of diffusion flames, a parameter called mixture fraction, denoted by Z in the case when the Lewis numbers of both the fuel and oxidizer are unity, is used. It is given by,

$$Z = \frac{\phi Y_F - (Y_O - 1)}{\phi + 1}, \quad (2.23)$$

In the case of the unequal Lewis number case, a parameter \hat{Z} called the modified mixture fraction is used. It is defined as follows

$$\hat{Z} = \frac{\Phi Y_F - (Y_O - 1)}{\Phi + 1}, \quad (2.24)$$

where,

$$\Phi = \phi \frac{\mathcal{L}_O}{\mathcal{L}_F}.$$

The mixture fractions are useful as we can eliminate the chemical reaction rate, ω , in the source terms of equations (2.19) and (2.20). Because ω is zero everywhere but tends to a very large value at the reaction sheet, the elimination of the reaction rate term in these equations makes their treatment easier. Under the assumption of infinite rate chemistry, the fuel and oxidizer are completely expended at the reaction sheet, i.e, $Y_F = Y_O = 0$ at the reaction sheet. Therefore, at the reaction sheet, Z and \hat{Z} take the values denoted as Z_{st} and \hat{Z}_{st} where the subscript 'st' refers to the stoichiometric

value. These are given by,

$$Z_{st} = \frac{1}{1 + \phi}, \quad (2.25)$$

for the unity Lewis numbers case and,

$$\hat{Z}_{st} = \frac{1}{1 + \Phi}, \quad (2.26)$$

for the unequal Lewis numbers case.

2.1 Boundary Conditions

The boundary conditions for the non-dimensional equations (2.15)-(2.20) are as follows:

On the left boundary, i.e, $x \rightarrow -\infty$,

$$T = 1, \quad (2.27)$$

$$Y_F = 1, \quad (2.28)$$

$$Y_O = 0. \quad (2.29)$$

On the right boundary, i.e, $x \rightarrow \infty$,

$$T = 1, \quad (2.30)$$

$$Y_F = 0, \quad (2.31)$$

$$Y_O = 1. \quad (2.32)$$

CHAPTER 3

WEAKLY CURVED FLAMES

3.1 Flow Field

In this study, we would like to investigate a counter flow diffusion flame when a flow field given by

$$V_1(x, y) = (x^2 - y^2, -2xy), \quad (3.1)$$

is superimposed on the already existing flow field described by (2.1). We have chosen this particular flow field because the 2^{nd} degree potential is the next order correction to potential flow and we intend to study the behavior of the reaction sheet subject to this flow field. The resulting flow field is given by $V(x, y) = (u, v)$, where u and v are,

$$u = -2x + \alpha(x^2 - y^2), \quad (3.2)$$

$$v = 2y - \alpha(2xy). \quad (3.3)$$

The resulting stream (ψ) and potential ($\bar{\phi}$, not to be confused with initial mixture strength, ϕ) functions are given by

$$\psi = -2xy + \alpha\left(x^2y - \frac{y^3}{3}\right), \quad (3.4)$$

$$\bar{\phi} = y^2 - x^2 + \alpha\left(\frac{x^3}{3} - xy^2\right). \quad (3.5)$$

The solution to $V(x, y) = 0$ lead us to the conclusion that there are two stagnation points in the flow field located at $(0, 0)$ and $(2/\alpha, 0)$. The corresponding pressure field, obtained by solving equations (2.15)-(2.17), is

$$p = -2(x^2 + y^2) + 2\alpha x(x^2 + y^2) - \frac{\alpha^2}{2}(x^2 + y^2)^2 \quad (3.6)$$

and

$$\frac{1}{y} \frac{\partial p}{\partial y} = 4 - 4\alpha x + 2\alpha^2(x^2 + y^2). \quad (3.7)$$

Sample flow fields for different α are given in Figure (3.1).

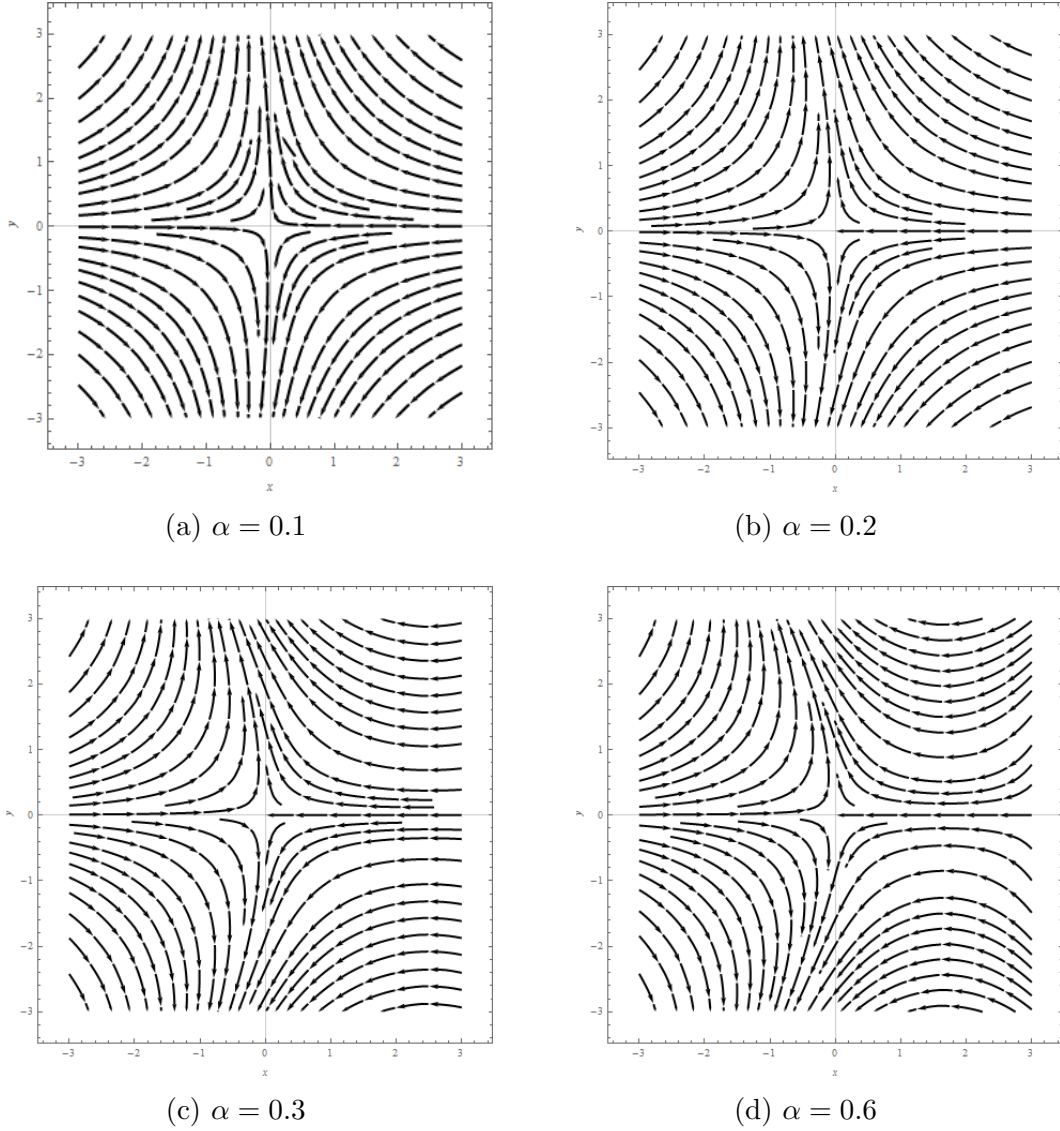


Figure 3.1: Flow Fields for different α

For simplicity, we assume $\alpha \ll 1$.

CHAPTER 4

UNITY LEWIS NUMBERS CASE

Let us consider the unity Lewis number case where $\mathcal{L}_F = \mathcal{L}_O = 1$. Along the y-direction, since the gradients are small, we introduce $\eta = \epsilon y$ such that $\epsilon = \alpha^{1/3}$ and $\epsilon \ll 1$, to magnify these gradients. The velocity components can thus be written as

$$u(x, \eta) = -2x - \epsilon\eta^2 + \epsilon^3 x^2 \sim -2x - \epsilon\eta^2 + \dots, \quad (4.1)$$

$$v(x, \eta) = \frac{1}{\epsilon} (2\eta - 2\epsilon^3 x\eta) \sim \frac{2\eta}{\epsilon}, \quad (4.2)$$

$$p(x, \eta) = -\frac{2}{\epsilon^2}\eta^2 - 2x^2 + 2\epsilon x\eta^2. \quad (4.3)$$

Using equations (2.19), (2.20), and (2.23), and assuming $\mathcal{L}_F = \mathcal{L}_O = 1$, we obtain,

$$u \frac{\partial Z}{\partial x} + v \frac{\partial Z}{\partial y} - \nabla^2 Z = 0. \quad (4.4)$$

The use of mixture fraction while dealing with the species equations eliminates the reaction rate term, ω , thus making the analysis a bit more easier.

The boundary conditions on Z , obtained using (2.28), (2.29), (2.31), and (2.32) are,

$$Z \rightarrow 1, \quad x \rightarrow -\infty, \quad (4.5)$$

$$Z \rightarrow 0, \quad x \rightarrow +\infty. \quad (4.6)$$

Let us assume the following asymptotic expansion for Z ,

$$Z(x, \eta) = Z^{(0)}(x) + \epsilon Z^{(1)}(x, \eta) + \mathcal{O}(\epsilon^2), \quad (4.7)$$

where $Z^{(0)}$ is the $\mathcal{O}(1)$ solution and $Z^{(1)}$ is the $\mathcal{O}(\epsilon)$ solution. Substituting this expansion into equation (4.4) using the fact that $y = \eta/\epsilon$ and u, v from

(4.1) and (4.2), the following equation is obtained,

$$2x \frac{dZ^{(0)}}{dx} + \frac{d^2 Z^{(0)}}{dx^2} + \epsilon \left(2x \frac{\partial Z^{(1)}}{\partial x} - 2\eta \frac{\partial Z^{(1)}}{\partial \eta} + \frac{\partial^2 Z^{(1)}}{\partial x^2} + \eta^2 \frac{dZ^{(0)}}{dx} \right) = 0.$$

Equating the $\mathcal{O}(1)$ and $\mathcal{O}(\epsilon)$ components on both LHS and RHS, the following two equations are obtained:

$$2x \frac{dZ^{(0)}}{dx} + \frac{d^2 Z^{(0)}}{dx^2} = 0, \quad (4.8)$$

$$2x \frac{\partial Z^{(1)}}{\partial x} - 2\eta \frac{\partial Z^{(1)}}{\partial \eta} + \frac{\partial^2 Z^{(1)}}{\partial x^2} = -\eta^2 \frac{dZ^{(0)}}{dx}. \quad (4.9)$$

Equation (4.8) corresponds to $\mathcal{O}(1)$ solution and equation (4.9) corresponds to the $\mathcal{O}(\epsilon)$ solution. The corresponding boundary conditions on $Z^{(0)}$ and $Z^{(1)}$ are,

$$Z^{(0)} = 1, \quad x \rightarrow -\infty, \quad (4.10)$$

$$Z^{(0)} = 0, \quad x \rightarrow +\infty, \quad (4.11)$$

$$Z^{(1)} = 0, \quad x \rightarrow \pm\infty. \quad (4.12)$$

It can be seen that (4.9) is symmetric with respect to the x-axis and we thus obtain the Neumann boundary condition,

$$\left. \frac{\partial Z^{(1)}}{\partial \eta} \right|_{\eta=0} = 0. \quad (4.13)$$

But, if we plug in $\eta = 0$ in (4.9), and solve it subject to the boundary conditions (4.12), we get the condition,

$$Z^{(1)}(x, 0) = 0, \quad (4.14)$$

which will serve as a Dirichlet boundary condition to solve (4.9). Solving equation (4.8) for $Z^{(0)}(x)$ subject to (4.10), we get

$$Z^{(0)}(x) = \frac{1}{2} \left[1 - \operatorname{erf}(x) \right], \quad (4.15)$$

where ‘ $\text{erf}(x)$ ’ is the error function defined as

$$\text{erf}(x) = \frac{2}{\sqrt{\pi}} \int_0^x e^{-t^2} dt.$$

Using (4.9) and (4.15), we get

$$2x \frac{\partial Z^{(1)}}{\partial x} - 2\eta \frac{\partial Z^{(1)}}{\partial \eta} + \frac{\partial^2 Z^{(1)}}{\partial x^2} = \frac{\eta^2}{\sqrt{\pi}} \exp(-x^2). \quad (4.16)$$

To solve the above equation, we assume the solution to be of the form,

$$Z^{(1)} = g(x) \eta^2, \quad (4.17)$$

where $g(x)$ is a function to be determined. This is a valid assumption because equation (4.16) is a linear partial differential equation and hence it must admit a solution of the form we have assumed. Further, to balance out the powers of η on both the LHS and RHS, $Z^{(1)}$ should vary as a second degree monomial in η . Substituting equation (4.17) into (4.16), we get the ordinary differential equation,

$$\frac{d^2 g}{dx^2} + 2x \frac{dg}{dx} - 4g = \frac{-\exp(-x^2)}{\sqrt{\pi}}. \quad (4.18)$$

Looking at the above equation, it can be assumed that the $g(x)$ is of the form,

$$g(x) = p(x) + k \exp(-x^2), \quad (4.19)$$

where k is constant to be determined and $p(x)$ is a function of x is also to be determined. $p(x)$ can be viewed as the homogeneous solution and $k \exp(-x^2)$ as the particular integral. Substituting (4.19) into (4.18) and comparing the coefficients of the resulting equation on the RHS and LHS, we get $k = -1/6\sqrt{\pi}$ and the equation,

$$\frac{d^2 p}{dx^2} + 2x \frac{dp}{dx} - 4p = 0. \quad (4.20)$$

subject to the boundary conditions,

$$p(x \rightarrow \pm\infty) = 0. \quad (4.21)$$

The solution of (4.20) can be shown to be,

$$p(x) = C_1 \exp(-x^2)H_{-3}(x) + C_2(2x^2 + 1), \quad (4.22)$$

where $H_n(x)$ is the n^{th} Hermite polynomial in x . Using the theory of Hermite polynomials, it can be shown that,

$$H_{-3}(x) = \frac{1}{8} \left[\left\{ \sqrt{\pi} \exp(x^2)(2x^2 + 1)(\text{erfc}(x)) \right\} - 2x \right]. \quad (4.23)$$

where $\text{erfc}(x)$ is the complementary error function defined as,

$$\text{erfc}(x) = 1 - \left\{ \frac{2}{\sqrt{\pi}} \int_0^x e^{-t^2} dt \right\}.$$

Clearly for $p(x)$ to be bounded when $x \rightarrow \pm\infty$, $C_1 = C_2 = 0$. Hence, the final solution is,

$$Z^{(1)}(x, \eta) = \frac{-\eta^2 \exp(-x^2)}{6\sqrt{\pi}} \quad (4.24)$$

The reader is encouraged to go through Appendix A, where the equation (4.16) has been solved numerically. Figure (A.2) shows the close match between the numerical and analytical results and thus reinforces the correctness of the analytical approach used to derive the result (4.24). The position of the reaction sheet where, $Y_F = Y_O = 0$ is determined by finding (x, η) corresponding to

$$Z(x, \eta) = Z_{st} = \frac{1}{1 + \phi}. \quad (4.25)$$

This position was identified earlier as $x_f(\eta)$. x_f can be expanded as

$$x_f = x_f^{(0)} + \epsilon\chi, \quad (4.26)$$

where $x_f^{(0)}$ and χ are the $\mathcal{O}(1)$ and $\mathcal{O}(\epsilon)$ components of the position of the reaction sheet respectively. We determine $x_f^{(0)}$ and $\chi(\eta)$ as follows:

Using equation (4.7) and (4.26), at a given η we can write,

$$Z(x_f, \eta) = Z^{(0)}(x_f^{(0)} + \epsilon\chi) + \epsilon Z^{(1)}(x_f^{(0)} + \epsilon\chi, \eta) = Z_{st}. \quad (4.27)$$

Expanding the terms using their corresponding Taylor expansions about $x_f^{(0)}$

we obtain,

$$Z^{(0)}(x_f) = Z^{(0)}(x_f^{(0)} + \epsilon\chi) = Z^{(0)}(x_f^{(0)}) + \epsilon\chi \left. \frac{dZ^{(0)}}{dx} \right|_{x_f^{(0)}} + \mathcal{O}(\epsilon^2), \quad (4.28)$$

$$Z^{(1)}(x_f) = Z^{(1)}(x_f^{(0)} + \epsilon\chi) = Z^{(1)}(x_f^{(0)}) + \epsilon\chi \left. \frac{\partial Z^{(1)}}{\partial x} \right|_{x_f^{(0)}} + \mathcal{O}(\epsilon^2) \quad (4.29)$$

Substituting the above expansions in (4.27)

$$\begin{aligned} Z^{(0)}(x_f^{(0)}) + \epsilon \left\{ \frac{dZ^{(0)}(x_f^{(0)})}{dx} \chi(\eta) + Z^{(1)}(x_f^{(0)}, \eta) \right\} + \dots \\ \dots + \epsilon^2 \left\{ \frac{\partial Z^{(1)}(x_f^{(0)}, \eta)}{\partial x} \chi(\eta) \right\} = Z_{st}. \end{aligned} \quad (4.30)$$

Equating the $\mathcal{O}(1)$ and $\mathcal{O}(\epsilon)$ parts on both the sides and ignoring the $\mathcal{O}(\epsilon^2)$, we obtain,

$$Z^{(0)}(x_f^{(0)}) = Z_{st}, \quad (4.31)$$

$$\frac{dZ^{(0)}(x_f^{(0)})}{dx} \chi(\eta) + Z^{(1)}(x_f^{(0)}, \eta) = 0. \quad (4.32)$$

Using (4.15), (4.25), and (4.31), we get,

$$x_f^{(0)} = \operatorname{erf}^{-1} \left(\frac{\phi - 1}{\phi + 1} \right) \quad (4.33)$$

Using (4.32), we get,

$$\chi(\eta) = - \frac{Z^{(1)}(x_f^{(0)}, \eta)}{\left(\frac{dZ^{(0)}(x_f^{(0)})}{dx} \right)} \quad (4.34)$$

Using (4.15) and (4.24) in (4.34), we get,

$$\chi(\eta) = - \frac{\eta^2}{6}. \quad (4.35)$$

Therefore, the position of the reaction sheet, x_f , is given by,

$$x_f = x_f^{(0)} - \frac{\epsilon\eta^2}{6}. \quad (4.36)$$

Using equation (3.5), it can be shown that there are three streamlines passing through the origin whose $\psi = 0$. Two of them are trivial and are the x and η axes. The third streamline is of more interest. Its equation is given by,

$$x = -\frac{\epsilon\eta^2}{6}. \quad (4.37)$$

This streamline is called the ‘seperatrix.’ It can be seen that the reaction sheet takes the exact shape of the seperatrix. Further, the reaction sheet is at a distance $x_f^{(0)}$ from the seperatrix.

Under the Burke-Schumann assumption, since there is no fuel in the oxidier region and vice-versa in the fuel region, using (4.7), (4.15) and (4.24), we can obtain the following distributions for Y_F and Y_O ,

$$Y_F = \begin{cases} 0, & Z \leq Z_{st} \\ \frac{Z-Z_{st}}{1-Z_{st}}, & Z \geq Z_{st}, \end{cases}$$

$$Y_O = \begin{cases} \frac{Z-Z_{st}}{Z_{st}}, & Z \leq Z_{st}, \\ 0, & Z \geq Z_{st}. \end{cases}$$

Alternatively, with the distribution of Z in the domain, the values of Z can be interpolated to find where $Z = Z_{st}$ occurs and the corresponding $x_f(\eta)$ are obtained. The x_f thus obtained is compared against the x_f obtained using the equations (4.33) and (4.34) in the Figure (4.1) for various ϵ .

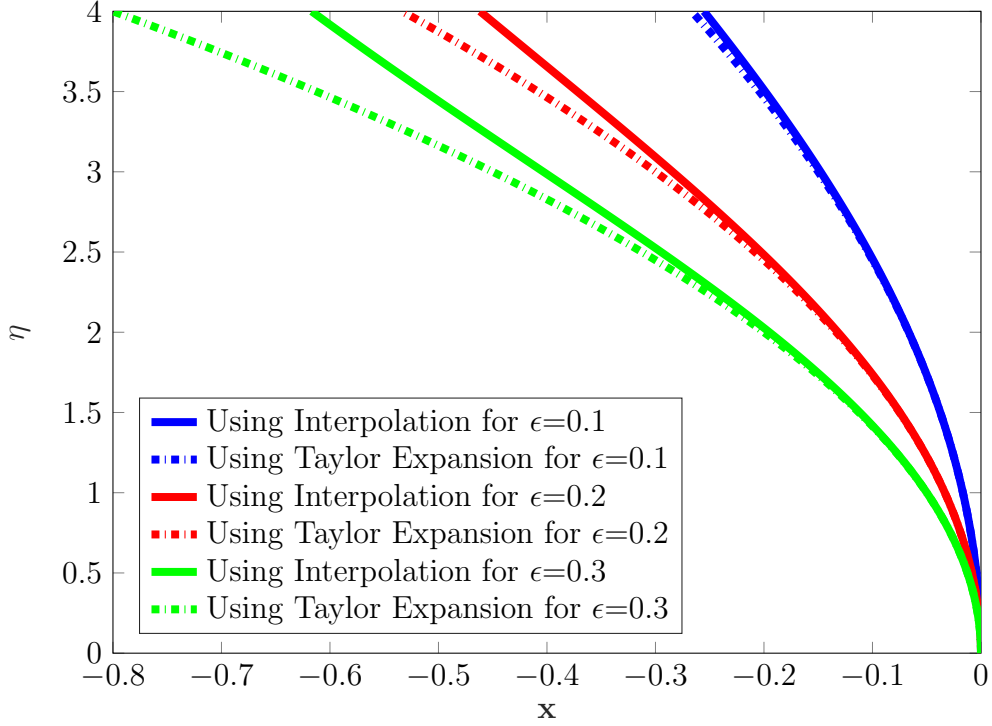


Figure 4.1: Comparison of Positions of Reaction Sheet using various approaches for $\phi = 1$

4.1 Temperature Distribution for Unity Lewis Numbers

The following method to evaluate the temperature distribution is only valid for unity Lewis numbers, i.e, only for $\mathcal{L}_F = \mathcal{L}_O = 1$. It is as follows:

Combining equations (2.19) and (2.20) by eliminating ω and molding the resultant in terms of Z , we obtain

$$u \frac{\partial Z}{\partial x} + v \frac{\partial Z}{\partial y} - \nabla^2 Z = 0, \quad (4.38)$$

Consider the energy and species equation of the fuel, (2.18) and (2.19), eliminating $q\omega$ and $-\omega$ from them, we obtain,

$$u(T + qY_F)_x + v(T + qY_F)_y - \nabla^2(T + qY_F) = 0, \quad (4.39)$$

where the subscripts x and y denote the partial derivatives with respect to x

and y respectively. Substituting $h_F = T + qY_F$ and $h_O = T + \frac{qY_O}{\phi}$, the above equation modifies into

$$u \frac{\partial h_F}{\partial x} + v \frac{\partial h_F}{\partial y} - \nabla^2 h_F = 0, \quad (4.40)$$

Equations (4.38) and (4.40) are similar but differ only in their boundary conditions and thus it can be assumed that there is a linear dependence between h_F and Z . Considering their corresponding boundary conditions, we obtain:

$$h_F = 1 + qZ, \quad (4.41)$$

$$h_O = 1 + \frac{q}{\phi}(1 - Z). \quad (4.42)$$

Since $Y_F = 0$ on the oxidizer side of the combustion system, h_F is essentially equal to the temperature in this region. Similar argument can be applied to h_O as well and hence the temperature distribution can be obtained as follows:

$$T = \begin{cases} 1 + qZ, & Z \leq Z_{st} \\ 1 + \frac{q}{\phi}(1 - Z), & Z \geq Z_{st}. \end{cases}$$

At $Z = Z_{st}$, i.e, at the reaction sheet, the temperature is maximum and is equal to the adiabatic temperature, denoted by T_a . It is given by

$$T_a = 1 + \frac{q}{1 + \phi}. \quad (4.43)$$

Adiabatic temperature decreases with increasing initial mixture strength, ϕ . It is interesting to note that this derivation is independent of the nature of the flow field as long as the assumptions of constant density and infinite rate chemistry hold. Further, the preceding derivation can be applied to the case where the Lewis numbers are equal but not necessarily unity with some modifications. This leads us to the conclusion that the temperature of the reaction sheet is constant as long as the Lewis numbers of the fuel and oxidizer are equal. It is to be noted that when the Lewis numbers are equal to unity, we refer to the temperature of the reaction sheet as the adiabatic temperature.

CHAPTER 5

UNEQUAL LEWIS NUMBERS CASE

Equation (2.19) is valid for $\hat{Z} > \hat{Z}_{st}$ which corresponds to the fuel zone while equation (2.20) is valid for $\hat{Z} < \hat{Z}_{st}$ which corresponds to the oxidizer zone. Using (2.24), we can combine (2.19) and (2.20) to get,

$$u \frac{\partial \hat{Z}}{\partial x} + v \frac{\partial \hat{Z}}{\partial y} = \frac{1}{\mathcal{L}} \nabla^2 \hat{Z}, \quad (5.1)$$

where,

$$\mathcal{L} = \mathcal{L}_F + \{\mathcal{L}_O - \mathcal{L}_F\} \bar{H}(\hat{Z}_{st} - \hat{Z}), \quad (5.2)$$

where $\bar{H}(x)$ is the Heaviside function defined as,

$$\bar{H}(x) = \begin{cases} 1, & x > 0, \\ 0, & x < 0. \end{cases}$$

We use a similar asymptotic expansion as was used in the equal Lewis number case and thus obtain,

$$\hat{Z}(x, \eta) = \hat{Z}^{(0)}(x) + \epsilon \hat{Z}^{(1)}(x, \eta) + \mathcal{O}(\epsilon^2), \quad (5.3)$$

where $\hat{Z}^{(0)}$ is the $\mathcal{O}(1)$ solution and $\hat{Z}^{(1)}$ is the $\mathcal{O}(\epsilon)$ solution. Plugging this into equation (5.1). Substituting $y = \eta/\epsilon$ and using u, v from (4.1) and (4.2), we get,

$$\begin{aligned} & (-2x - \epsilon\eta^2) \frac{\partial(\hat{Z}^{(0)} + \epsilon\hat{Z}^{(1)})}{\partial x} + \frac{2\eta}{\epsilon} \frac{\partial(\hat{Z}^{(0)} + \epsilon\hat{Z}^{(1)})}{\partial y} + \dots \\ & \dots + \frac{1}{\mathcal{L}} \left\{ \frac{\partial^2(\hat{Z}^{(0)} + \epsilon\hat{Z}^{(1)})}{\partial x^2} + \frac{\partial^2(\hat{Z}^{(0)} + \epsilon\hat{Z}^{(1)})}{\partial y^2} \right\} = 0. \end{aligned} \quad (5.4)$$

Using binomial expansion, we can expand the Heaviside function in (5.2) as,

$$\begin{aligned}
& \bar{H}(\hat{Z}_{st} - \hat{Z}) = \bar{H}(\hat{Z}_{st} - \{\hat{Z}^{(0)} + \epsilon \hat{Z}^{(1)}\}), \\
& \implies \bar{H}(\hat{Z}_{st} - \hat{Z}) = \bar{H}(\hat{Z}_{st} - \hat{Z}^{(0)}) + \epsilon \hat{Z}^{(1)} \delta(\hat{Z}_{st} - \hat{Z}^{(0)}), \\
& \implies \mathcal{L} = \mathcal{L}_F + [(\mathcal{L}_O - \mathcal{L}_F)\{\bar{H}(\hat{Z}_{st} - \hat{Z}^{(0)}) + \epsilon \hat{Z}^{(1)} \delta(\hat{Z}_{st} - \hat{Z}^{(0)})\}],
\end{aligned}$$

where $\delta(x)$ is the Dirac-delta distribution, defined as,

$$\delta(x) = \begin{cases} \infty, & x = 0, \\ 0, & x \neq 0. \end{cases}$$

Using the above result in (5.4) and filtering the $\mathcal{O}(1)$ and $\mathcal{O}(\epsilon)$ components, we get,

$$2x \frac{d\hat{Z}^{(0)}}{dx} + \frac{1}{\mathcal{L}^{(0)}} \frac{d^2 \hat{Z}^{(0)}}{dx^2} = 0, \quad (5.5)$$

$$\begin{aligned}
& 2x \hat{Z}^{(1)} (\mathcal{L}_F - \mathcal{L}_O) \mathcal{L}^{(0)} \delta(\hat{Z}^{(0)} - \hat{Z}_{st}) \frac{d\hat{Z}^{(0)}}{dx} + 2x \mathcal{L}^{(0)} \frac{\partial \hat{Z}^{(1)}}{\partial x} + \dots \\
& \dots - 2\eta \mathcal{L}^{(0)} \frac{\partial \hat{Z}^{(1)}}{\partial \eta} + \frac{\partial^2 \hat{Z}^{(1)}}{\partial x^2} = -\eta^2 \mathcal{L}^{(0)} (\hat{Z}^{(0)}) \frac{d\hat{Z}^{(0)}}{dx},
\end{aligned} \quad (5.6)$$

where

$$\mathcal{L}^{(0)} = \mathcal{L}_F + \{\mathcal{L}_O - \mathcal{L}_F\} \bar{H}(\hat{Z}_{st} - \hat{Z}^{(0)}),$$

The corresponding boundary conditions on $\hat{Z}^{(0)}$ and $\hat{Z}^{(1)}$ are

$$\hat{Z}^{(0)} = 1, \quad x \rightarrow -\infty, \quad (5.7)$$

$$\hat{Z}^{(0)} = 0, \quad x \rightarrow +\infty, \quad (5.8)$$

$$\hat{Z}^{(1)} = 0, \quad x \rightarrow \pm\infty, \quad (5.9)$$

$$\hat{Z}^{(1)}(x, 0) = 0. \quad (5.10)$$

While solving (5.6), we run into the trouble in the first term since this turns out to be a product of a dirac-delta distribution and Heaviside function which is undefined. To overcome this, we define a boundary condition at $x = x_f^{(0)}$

and split the equation into two parts,

$$\begin{cases} 2x \frac{\partial \hat{Z}^{(1)}}{\partial x} - 2\eta \frac{\partial \hat{Z}^{(1)}}{\partial \eta} + \frac{1}{\mathcal{L}_F} \frac{\partial^2 \hat{Z}^{(1)}}{\partial x^2} = -\eta^2 \frac{d\hat{Z}^{(0)}}{dx}, & x < x_f^{(0)}, \\ 2x \frac{\partial \hat{Z}^{(1)}}{\partial x} - 2\eta \frac{\partial \hat{Z}^{(1)}}{\partial \eta} + \frac{1}{\mathcal{L}_O} \frac{\partial^2 \hat{Z}^{(1)}}{\partial x^2} = -\eta^2 \frac{d\hat{Z}^{(0)}}{dx}, & x > x_f^{(0)}. \end{cases} \quad (5.11)$$

The boundary condition at $x = x_f^{(0)}$ is derived as follows:

We know that at $x_f = x_f^{(0)} + \epsilon\chi$,

$$\hat{Z}(x_f, \eta) = \hat{Z}_{st} = \frac{1}{1 + \Phi}, \quad (5.12)$$

By Taylor expansion,

$$\left\{ \hat{Z} + \epsilon\chi \frac{\partial \hat{Z}}{\partial x} \right\} \Big|_{x_f^{(0)}} = \frac{1}{1 + \Phi}. \quad (5.13)$$

Using (5.3) in the above equation, we get,

$$\begin{aligned} \hat{Z}^{(0)}(x_f^{(0)}) + \epsilon \left\{ \hat{Z}^{(1)} + \chi \frac{d\hat{Z}^{(0)}}{dx} \right\} \Big|_{x_f^{(0)}} &= \frac{1}{1 + \Phi}, \\ \implies \hat{Z}^{(1)}(x_f^{(0)}) &= -\chi \frac{d\hat{Z}^{(0)}}{dx} \Big|_{x_f^{(0)}} \end{aligned} \quad (5.14)$$

Considering the fact that the Lewis number distribution is discontinuous, the boundary conditions have to be supplemented with appropriate jump conditions in $\hat{Z}^{(0)}$ and $\hat{Z}^{(1)}$. They are derived as follows:

Consider the jump condition,

$$[[\hat{Z}]]_{x_f} = 0.$$

Using (5.3) and by expanding the terms using a Taylor expansion about

$x = x_f^{(0)}$, we get,

$$[[\hat{Z}]]_{x_f} = [[\hat{Z}^{(0)} + \epsilon \hat{Z}^{(1)}]]_{x_f} = 0, \quad (5.15)$$

$$\implies [[\hat{Z}]]_{x_f} = \left[\hat{Z}^{(0)} + \epsilon \left\{ \hat{Z}^{(1)} + \frac{d\hat{Z}^{(0)}}{dx} \right\} + \epsilon^2 \frac{\partial \hat{Z}^{(1)}}{\partial x} \right]_{x_f^{(0)}} = 0, \quad (5.16)$$

Filtering the $\mathcal{O}(1)$ and $\mathcal{O}(\epsilon)$ components, we get the jump conditions,

$$[[\hat{Z}^{(0)}]]_{x_f^{(0)}} = 0, \quad (5.17)$$

$$[[\hat{Z}^{(1)}]]_{x_f^{(0)}} = -\chi \left[\left[\frac{d\hat{Z}^{(0)}}{dx} \right] \right]_{x_f^{(0)}}. \quad (5.18)$$

Across the reaction sheet, we have the jump condition,

$$\frac{1}{\mathcal{L}_F} \left[\left[\frac{\partial Y_F}{\partial n} \right] \right]_{x_f} = \frac{1}{\phi \mathcal{L}_O} \left[\left[\frac{\partial Y_O}{\partial n} \right] \right]_{x_f}, \quad (5.19)$$

The derivative across the normal to the reaction sheet can be evaluated as follows:

$$\frac{\partial}{\partial n} = \hat{n} \cdot \nabla, \quad (5.20)$$

where \hat{n} is the unit vector along the normal to the reaction sheet. Since the position of the reaction sheet is given by $x_f = x_f^{(0)} + \epsilon \chi(\eta)$ from (4.26), \hat{n} is given by

$$\hat{n} = \left(\frac{1, -\epsilon \chi'}{\sqrt{1 + \epsilon^2 \chi'^2}} \right), \quad (5.21)$$

where $\chi' = \frac{\partial \chi}{\partial x}$. Since $\epsilon^2 \chi'^2$ is $\mathcal{O}(\epsilon^2)$, it can be ignored,

$$\implies \frac{\partial}{\partial n} \approx \frac{\partial}{\partial x} - \epsilon \chi' \frac{\partial}{\partial \eta}. \quad (5.22)$$

The equation (5.19) can be recast as,

$$\left[\left[\frac{\partial \hat{Z}}{\partial n} \right] \right]_{x_f} = 0. \quad (5.23)$$

Using (5.22) in the above equation, we get,

$$\left[\left[\frac{\partial \hat{Z}}{\partial x} - \epsilon \chi' \frac{\partial \hat{Z}}{\partial \eta} \right] \right]_{x_f} = 0,$$

Using (5.3) into the above equation,

$$\left[\left[\frac{d\hat{Z}^{(0)}}{dx} + \epsilon \frac{\partial \hat{Z}^{(1)}}{\partial x} - \epsilon^2 \chi \frac{\partial \hat{Z}^{(1)}}{\partial \eta} \right] \right]_{x_f} = 0 \quad (5.24)$$

Ignoring the $\mathcal{O}(\epsilon^2)$ component and expanding the terms by a Taylor expansion about $x = x_f^{(0)}$,

$$\left[\left[\frac{d\hat{Z}^{(0)}}{dx} + \epsilon \left\{ \chi \frac{d^2 \hat{Z}^{(0)}}{dx^2} + \frac{\partial \hat{Z}^{(1)}}{\partial x} \right\} \right] \right]_{x_f^{(0)}} = 0$$

Equating the $\mathcal{O}(1)$ and $\mathcal{O}(\epsilon)$ components to the RHS, we get the jump conditions ,

$$\left[\left[\frac{d\hat{Z}^{(0)}}{dx} \right] \right]_{x_f^{(0)}} = 0, \quad (5.25)$$

$$\left[\left[\frac{\partial \hat{Z}^{(1)}}{\partial x} \right] \right]_{x_f^{(0)}} = -\chi \left[\left[\frac{d^2 \hat{Z}^{(0)}}{dx^2} \right] \right]_{x_f^{(0)}}. \quad (5.26)$$

We can derive an equation for χ similar to (4.34) for \hat{Z} which turns out to be

$$\chi = \frac{-\hat{Z}^{(1)}(x_f^{(0)})}{\left(\frac{d\hat{Z}^{(0)}(x_f^{(0)})}{dx} \right)}. \quad (5.27)$$

The solution for (5.5) using the boundary conditions (5.7), (5.8) and jump conditions (5.25) and (5.17) is

$$\hat{Z}^{(0)}(x) = \begin{cases} 1 - \left[\frac{\Phi}{1+\Phi} \frac{1+\text{erf}(\sqrt{\mathcal{L}_F} x)}{1+\text{erf}(\sqrt{\mathcal{L}_F} x_f^{(0)})} \right], & x \leq x_f^{(0)} \\ \frac{1}{1+\Phi} \frac{1-\text{erf}(\sqrt{\mathcal{L}_O} x)}{1-\text{erf}(\sqrt{\mathcal{L}_O} x_f^{(0)})}, & x \geq x_f^{(0)}. \end{cases} \quad (5.28)$$

Using (5.25), we obtain the following implicit equation in $x_f^{(0)}$ which can be solved to get $x_f^{(0)}$,

$$\frac{1 + \operatorname{erf}(\sqrt{\mathcal{L}_F} x_f^{(0)})}{1 - \operatorname{erf}(\sqrt{\mathcal{L}_O} x_f^{(0)})} = \Phi \sqrt{\frac{\mathcal{L}_F}{\mathcal{L}_O}} \exp \{(\mathcal{L}_O - \mathcal{L}_F)(x_f^{(0)})^2\}. \quad (5.29)$$

To solve (5.6), we assume a solution of the form,

$$\hat{Z}^{(1)} = \begin{cases} f_1(x)g_1(\eta), & x \leq x_f^{(0)}, \\ f_2(x)g_2(\eta), & x \geq x_f^{(0)}, \end{cases} \quad (5.30)$$

This is a valid assumption because (5.6) is a linear partial differential equation in $\hat{Z}^{(1)}$. Further, to balance the terms containing η on the LHS and RHS of (5.6), $g_1(\eta) = g_2(\eta) = \eta^2$. Considering (5.28), we can deduce that

$$\chi = k\eta^2 \quad (5.31)$$

where ‘ k ’ is an unknown. We solve (5.6) numerically as shown in Appendix B. Using a methodology similar to the one used to solve (4.16), we get the analytical solution for (5.6) to be,

$$\hat{Z}^1(x, \eta) = \begin{cases} -\frac{1}{3\sqrt{\pi}} \frac{\Phi}{1+\Phi} \frac{\sqrt{\mathcal{L}_F} \eta^2 \exp(-x^2 \mathcal{L}_F)}{1 + \operatorname{erf}(\sqrt{\mathcal{L}_F} x_f^{(0)})}, & x \leq x_f^{(0)}, \\ -\frac{1}{3\sqrt{\pi}} \frac{1}{1+\Phi} \frac{\sqrt{\mathcal{L}_O} \eta^2 \exp(-x^2 \mathcal{L}_O)}{1 - \operatorname{erf}(\sqrt{\mathcal{L}_O} x_f^{(0)})}, & x \geq x_f^{(0)} \end{cases} \quad (5.32)$$

The reader is encouraged to go through Appendix B to explore the numerical methodology to solve equation (5.11).

Using the above equation, we get,

$$\chi = \frac{-\eta^2}{6}. \quad (5.33)$$

It is to be noted that the $k \approx -0.1667$ for the above equation—which matches the one obtained numerically solving for k using the methodology based on Appendix B. With information about \hat{Z} , the individual distribution of Y_F and Y_O can be obtained as follows,

$$Y_F(x, \eta) = \frac{\hat{Z} - \hat{Z}_{st}}{1 - \hat{Z}_{st}} \bar{H}(\hat{Z}_{st} - \hat{Z}) = \frac{\hat{Z}(1 + \Phi) - 1}{\Phi} \bar{H}(\hat{Z}_{st} - \hat{Z}), \quad (5.34)$$

$$Y_O(x, \eta) = \frac{\hat{Z}_{st} - \hat{Z}}{\hat{Z}_{st}} \bar{H}(\hat{Z} - \hat{Z}_{st}) = \{1 - \hat{Z}(1 + \Phi)\} \bar{H}(\hat{Z} - \hat{Z}_{st}), \quad (5.35)$$

CHAPTER 6

TEMPERATURE DISTRIBUTION IN UNEQUAL LEWIS NUMBER CASE

Consider (2.18), under the Burke-Schumann limit, the equation modifies into,

$$u \frac{\partial T}{\partial x} + v \frac{\partial T}{\partial y} - \nabla^2 T = \begin{cases} 0, & x \leq x_f, \\ 0, & x \geq x_f. \end{cases} \quad (6.1)$$

Using a similar perturbation approach as was used for Z and \hat{Z} , we introduce,

$$T(x, \eta) = T^{(0)}(x) + \epsilon T^{(1)}(x, \eta) + \mathcal{O}(\epsilon^2), \quad (6.2)$$

where $T^{(0)}$ is the solution of $\mathcal{O}(1)$ and $T^{(1)}$ is the $\mathcal{O}(\epsilon)$ solution. Plugging this into equation (6.1) and by substituting $y = \eta/\epsilon$ and using u, v from (4.1) and (4.2) and then filtering the $\mathcal{O}(1)$ and $\mathcal{O}(\epsilon)$ components, we have the $\mathcal{O}(1)$ and $\mathcal{O}(\epsilon)$ equations for T as,

$$2x \frac{dT^{(0)}}{dx} + \frac{d^2 T^{(0)}}{dx^2} = \begin{cases} 0, & x \leq x_f^{(0)}, \\ 0, & x \geq x_f^{(0)}. \end{cases} \quad (6.3)$$

$$2x \frac{\partial T^{(1)}}{\partial x} - 2\eta \frac{\partial T^{(1)}}{\partial \eta} + \frac{\partial^2 T^{(1)}}{\partial x^2} = \begin{cases} -\eta^2 \frac{dT^{(0)}}{dx}, & x \leq x_f^{(0)}, \\ -\eta^2 \frac{dT^{(0)}}{dx}, & x \geq x_f^{(0)}. \end{cases} \quad (6.4)$$

The corresponding boundary conditions on $T^{(0)}$ and $T^{(1)}$ are

$$T^{(0)} = 1, \quad x \rightarrow -\infty, \quad (6.5)$$

$$T^{(0)} = 1, \quad x \rightarrow +\infty, \quad (6.6)$$

$$T^{(1)} = 0, \quad x \rightarrow \pm\infty, \quad (6.7)$$

$$T^{(1)}(x, 0) = 0. \quad (6.8)$$

In addition to the boundary conditions, we have to supply jump conditions in $T^{(0)}$ and $T^{(1)}$ which are derived as follows:

The temperature is continuous across the reaction sheet, hence

$$\llbracket T \rrbracket_{x_f} = 0. \quad (6.9)$$

Substituting (6.2) and expanding the above equation about $x_f^{(0)}$ using Taylor's expansion as follows :

$$\left[\left[T^{(0)} + \epsilon \left(\chi \frac{dT^{(0)}}{dx} + T^{(1)} \right) \right] \right]_{x_f^{(0)}} = 0 \quad (6.10)$$

Considering only the $\mathcal{O}(\infty)$ component of the above equation, we have,

$$\llbracket T^{(0)} \rrbracket_{x_f^{(0)}} = 0, \quad (6.11)$$

$$\llbracket T^{(1)} \rrbracket_{x_f^{(0)}} = -\chi \left[\left[\frac{dT^{(0)}}{dx} \right] \right]_{x_f^{(0)}}. \quad (6.12)$$

In addition, we know that across the reaction sheet,

$$\left[\left[\frac{\partial T}{\partial n} \right] \right]_{x_f} = -\frac{q}{\mathcal{L}_F} \left[\left[\frac{\partial Y_F}{\partial n} \right] \right]_{x_f}, \quad (6.13)$$

where n is the local normal to the reaction sheet. Further, using (5.22), we get,

$$\left[\left[\frac{\partial T}{\partial x} - \epsilon \chi \frac{\partial T}{\partial \eta} \right] \right]_{x_f} = -\frac{q}{\mathcal{L}_F} \left[\left[\frac{\partial Y_F}{\partial x} - \epsilon \chi \frac{\partial Y_F}{\partial \eta} \right] \right]_{x_f} \quad (6.14)$$

Consider,

$$Y_F = \frac{\hat{Z} - \hat{Z}_{st}}{1 - \hat{Z}_{st}} \bar{H}(\hat{Z} - \hat{Z}_{st}), \quad (6.15)$$

Using $Y_F = Y_F^{(0)} + \epsilon Y_F^{(1)}$ and (5.3),

$$Y_F^{(0)} + \epsilon Y_F^{(1)} = \frac{\hat{Z}^{(0)} - \hat{Z}_{st} + \epsilon \hat{Z}^{(1)}}{1 - \hat{Z}_{st}} \bar{H}(\hat{Z}^{(0)} - \hat{Z}_{st} + \epsilon \hat{Z}^{(1)}), \quad (6.16)$$

$$\begin{aligned} \implies Y_F^{(0)} + \epsilon Y_F^{(1)} = & \left\{ \frac{\hat{Z}^{(0)} - \hat{Z}_{st}}{1 - \hat{Z}_{st}} + \frac{\epsilon \hat{Z}^{(1)}}{1 - \hat{Z}_{st}} \right\} \left\{ \bar{H}(\hat{Z}^{(0)} - \hat{Z}_{st}) + \dots \right. \\ & \left. \dots + \epsilon \hat{Z}^{(1)} \delta(\hat{Z}^{(0)} - \hat{Z}_{st}) \right\}, \end{aligned} \quad (6.17)$$

$$\begin{aligned} \implies Y_F^{(0)} + \epsilon Y_F^{(1)} = & \frac{\hat{Z}^{(0)} - \hat{Z}_{st}}{1 - \hat{Z}_{st}} \bar{H}(\hat{Z}^{(0)} - \hat{Z}_{st}) + \dots \\ & \dots + \epsilon \left\{ \frac{\hat{Z}^{(1)}}{1 - \hat{Z}_{st}} \bar{H}(\hat{Z}^{(0)} - \hat{Z}_{st}) \right\} + \mathcal{O}(\epsilon^2). \end{aligned} \quad (6.18)$$

We can equate the $\mathcal{O}(1)$ and $\mathcal{O}(\epsilon)$ components on both sides to get,

$$Y_F^{(0)} = \frac{\hat{Z}^{(0)} - \hat{Z}_{st}}{1 - \hat{Z}_{st}} \bar{H}(\hat{Z}^{(0)} - \hat{Z}_{st}), \quad (6.19)$$

$$Y_F^{(1)} = \frac{\hat{Z}^{(1)}}{1 - \hat{Z}_{st}} \bar{H}(\hat{Z}^{(0)} - \hat{Z}_{st}). \quad (6.20)$$

Now,

$$\left[\left[\frac{\partial Y_F}{\partial x} \right] \right]_{x_f} = \left[\left[\frac{dY_F^{(0)}}{dx} + \epsilon \frac{\partial Y_F^{(1)}}{\partial x} \right] \right]_{x_f} \quad (6.21)$$

Using the fact that $x_f = x_f^{(0)} + \epsilon \chi$ and doing a Taylor expansion about $x = x_f^{(0)}$,

$$\left[\left[\frac{\partial Y_F}{\partial x} \right] \right]_{x_f} = \left[\left[\frac{dY_F^{(0)}}{dx} + \epsilon \left\{ \frac{\partial Y_F^{(1)}}{\partial x} + \chi \frac{d^2 Y_F^{(0)}}{dx^2} \right\} \right] \right]_{x_f^{(0)}} \quad (6.22)$$

Using (5.28), (5.32), (6.19) and (6.20), we can deduce that,

$$\left[\left[\frac{\partial Y_F^{(1)}}{\partial x} + \chi \frac{d^2 Y_F^{(0)}}{dx^2} \right] \right]_{x_f^{(0)}} = 0. \quad (6.23)$$

Using (6.2) in (6.14), we get,

$$\left[\left[\frac{d\Gamma^{(0)}}{dx} + \epsilon \frac{\partial \Gamma^{(1)}}{\partial x} - \epsilon^2 \chi \frac{\partial \Gamma^{(1)}}{\partial \eta} \right] \right]_{x_f} = -\frac{q}{\mathcal{L}_F} \left[\left[\frac{dY_F^{(0)}}{dx} + \epsilon \frac{\partial Y_F^{(1)}}{\partial x} - \epsilon^2 \chi \frac{\partial Y_F^{(1)}}{\partial \eta} \right] \right]_{x_f} \quad (6.24)$$

Ignoring the $\mathcal{O}(\epsilon^2)$ terms,

$$\left[\frac{dT^{(0)}}{dx} + \epsilon \frac{\partial T^{(1)}}{\partial x} \right]_{x_f} = -\frac{q}{\mathcal{L}_F} \left[\frac{dY_F^{(0)}}{dx} + \epsilon \frac{\partial Y_F^{(1)}}{\partial x} \right]_{x_f} \quad (6.25)$$

Taking the Taylor expansion about $x_f^{(0)}$,

$$\left[\frac{dT^{(0)}}{dx} + \epsilon \left(\chi \frac{d^2 T^{(0)}}{dx^2} + \frac{\partial T^{(1)}}{\partial x} \right) \right]_{x_f^{(0)}} = -\frac{q}{\mathcal{L}_F} \left[\frac{dY_F^{(0)}}{dx} + \epsilon \left(\chi \frac{d^2 Y_F^{(0)}}{dx^2} + \frac{\partial Y_F^{(1)}}{\partial x} \right) \right]_{x_f^{(0)}}. \quad (6.26)$$

Using (6.23) in the above equation, we can derive the jump conditions,

$$\left[\frac{dT^{(0)}}{dx} \right]_{x_f^{(0)}} = -\frac{q}{\mathcal{L}_F} \left[\frac{dY_F^{(0)}}{dx} \right]_{x_f^{(0)}}, \quad (6.27)$$

$$\left[\frac{\partial T^{(1)}}{\partial x} \right]_{x_f^{(0)}} = -\chi \left[\frac{d^2 T^{(0)}}{dx^2} \right]_{x_f^{(0)}} \quad (6.28)$$

. With (6.11) and (6.27), the equation (6.3) is now closed and can be solved analytically to obtain the following result,

$$T^{(0)} = \begin{cases} 1 + \frac{1+\text{erf}(x)}{1+\text{erf}(x_f^{(0)})} (T_s - 1), & x \leq x_f^{(0)}, \\ 1 + \frac{1-\text{erf}(x)}{1-\text{erf}(x_f^{(0)})} (T_s - 1), & x \geq x_f^{(0)}, \end{cases} \quad (6.29)$$

where,

$$T_s = 1 + \frac{q}{2\sqrt{\mathcal{L}_F}} \exp\{(1 - \mathcal{L}_F)(x_f^{(0)})^2\} \frac{1 - \text{erf}^2(x_f^{(0)})}{1 + \text{erf}(\sqrt{\mathcal{L}_F} x_f^{(0)})}.$$

Using (6.12), (6.28) we can solve (6.4) for $T^{(1)}$ to get,

$$T^{(1)}(x, \eta) = \begin{cases} \frac{1}{3\sqrt{\pi}} \frac{(T_s - 1)\eta^2 e^{-x^2}}{1 + \text{erf}(x_f^{(0)})}, & x \leq x_f^{(0)}, \\ \frac{-1}{3\sqrt{\pi}} \frac{(T_s - 1)\eta^2 e^{-x^2}}{1 - \text{erf}(x_f^{(0)})}, & x \geq x_f^{(0)}. \end{cases} \quad (6.30)$$

Now that we know $T^{(0)}$ and $T^{(1)}$, we can find the temperature of the reaction

sheet, $T(x_f)$ as follows:

$$T(x_f) = T^{(0)}(x_f^{(0)}) + \epsilon \left\{ \chi \frac{dT^{(0)}}{dx} \Big|_{x_{f\pm}^{(0)}} + T^{(1)}(x_{f\pm}^{(0)}) \right\},$$

$$\implies T(x_f) = T_s \tag{6.31}$$

Thus, we have shown that the temperature of the reaction sheet for the unequal Lewis numbers case is constant and is equal to the stoichiometric temperature.

Alternatively, the equation (6.4) was solved numerically using the Immersed Interface Method (IIM) based on Li and Ito (2006) the algorithm of which is given in Appendix C. The correctness of analytical solution is compared against the numerical results by performing a Grid Dependency Test, the results of which have been shown in Figure (C.2) in Appendix C.

CHAPTER 7

RESULTS

7.1 Unity Lewis Numbers Case

In this section, the plots of $Z^{(0)}$, $Z^{(1)}$, $T^{(0)}$, and $T^{(1)}$ are presented for the combinations of \mathcal{L}_F , \mathcal{L}_O and ϕ given in Table 7.2.

\mathcal{L}_F	\mathcal{L}_O	ϕ	q	$x_f^{(0)}$
1	1	0.5	6	-0.3046
1	1	1	6	0
1	1	2	6	0.3046

Table 7.1: Combinations of physical parameters considered for the unequal Lewis numbers case

Further, the dimensions of the domain considered are as follows:

Length of the domain along the x-direction, $L=16$.

Height of the domain along the η -direction, $W= 2$.

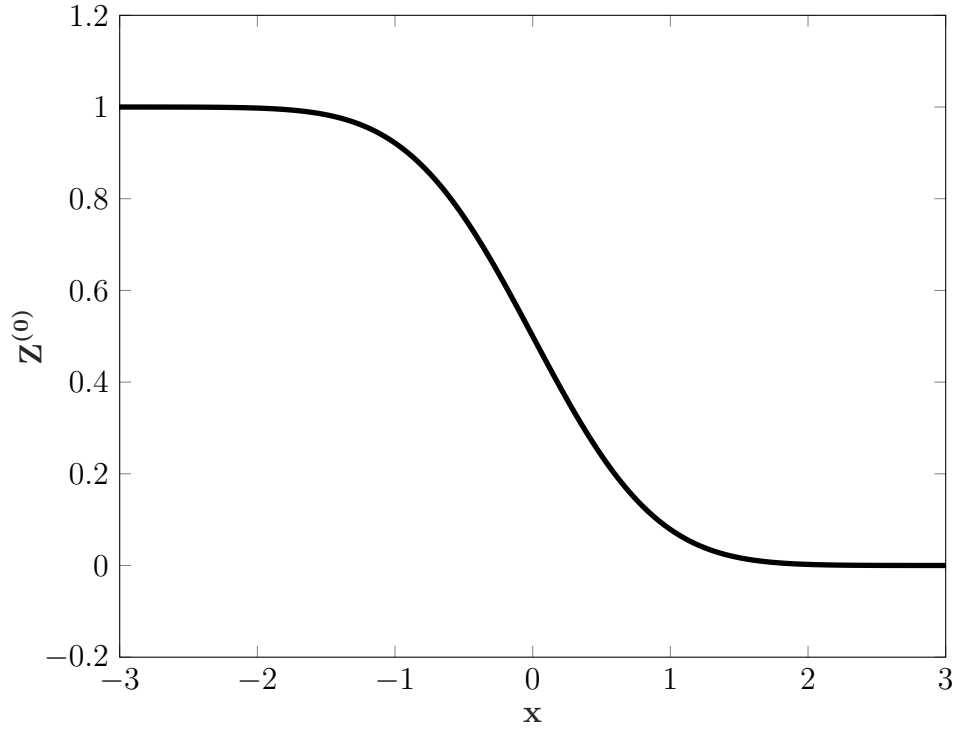


Figure 7.1: Variation of $\hat{Z}^{(0)}$ for $\mathcal{L}_F=1$, $\mathcal{L}_O=1$ and $\phi=0.5$

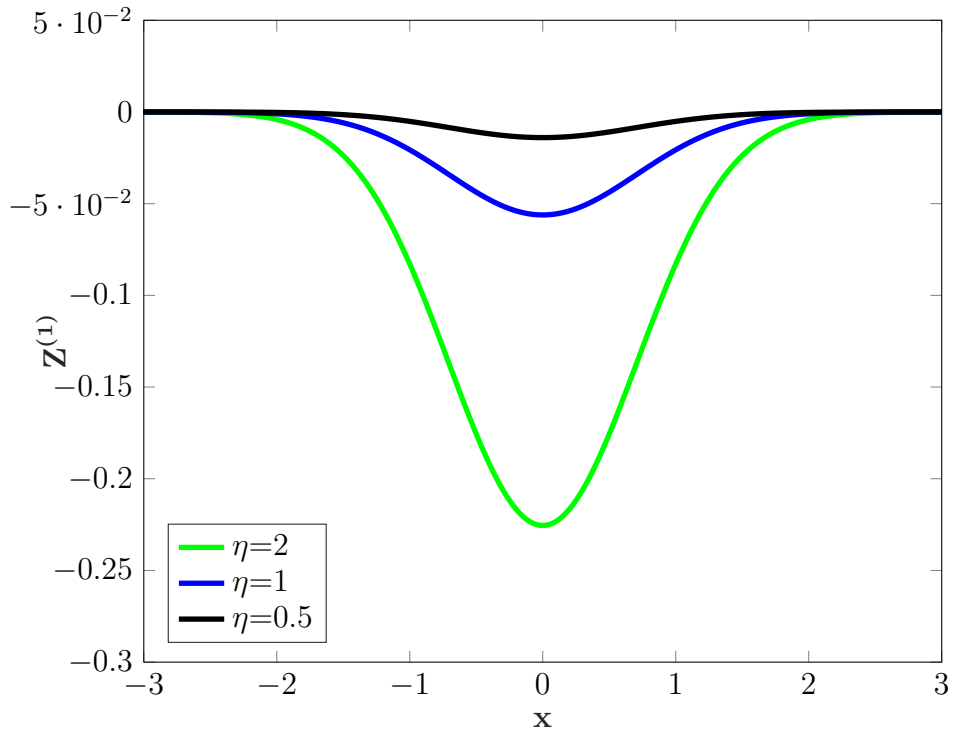


Figure 7.2: Variation of $\hat{Z}^{(1)}$ for $\mathcal{L}_F=1$, $\mathcal{L}_O=1$ and $\phi=0.5$

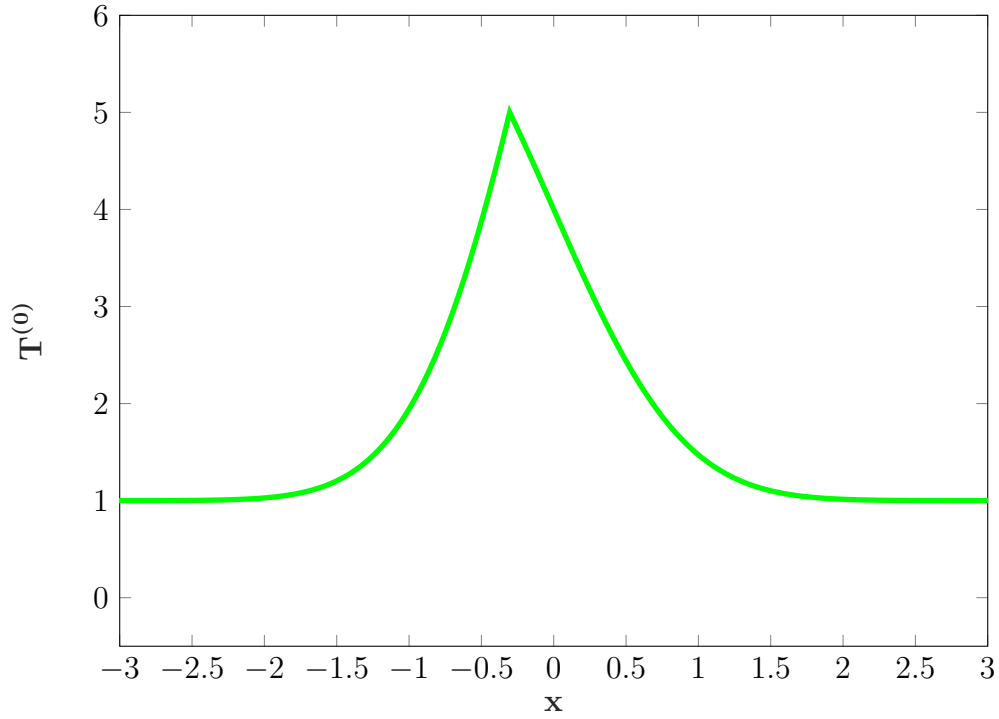


Figure 7.3: Variation of $T^{(0)}$ for $\mathcal{L}_F=1$, $\mathcal{L}_O=1$ and $\phi=0.5$

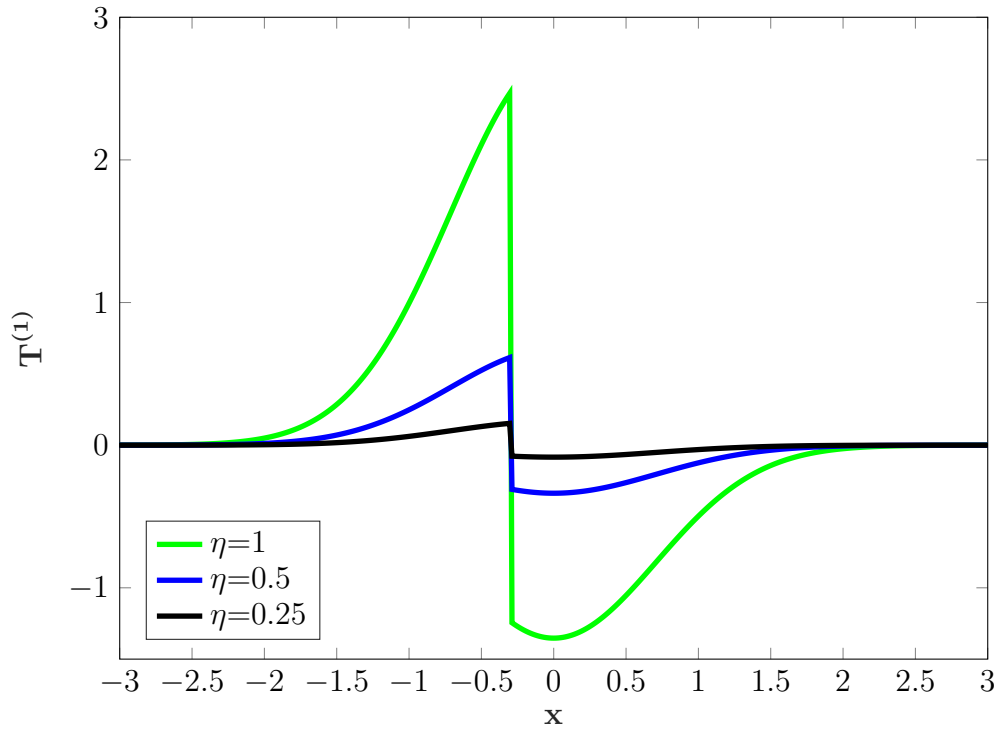


Figure 7.4: Variation of $T^{(1)}$ for $\mathcal{L}_F=1$, $\mathcal{L}_O=1$ and $\phi=0.5$

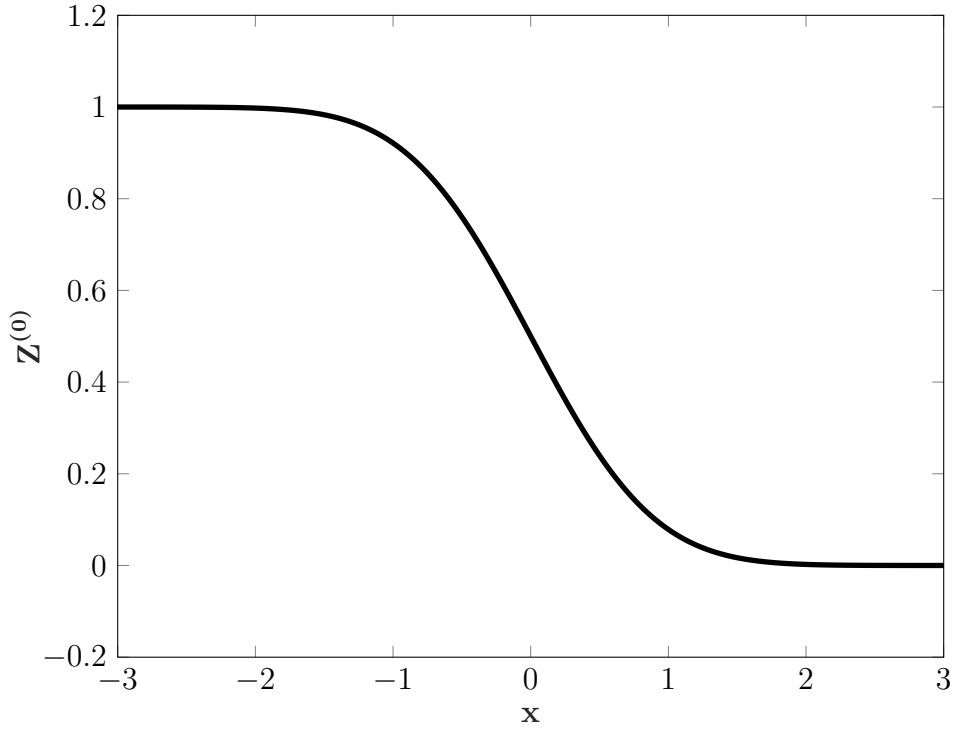


Figure 7.5: Variation of $\hat{Z}^{(0)}$ for $\mathcal{L}_F=1$, $\mathcal{L}_O=1$ and $\phi=1$

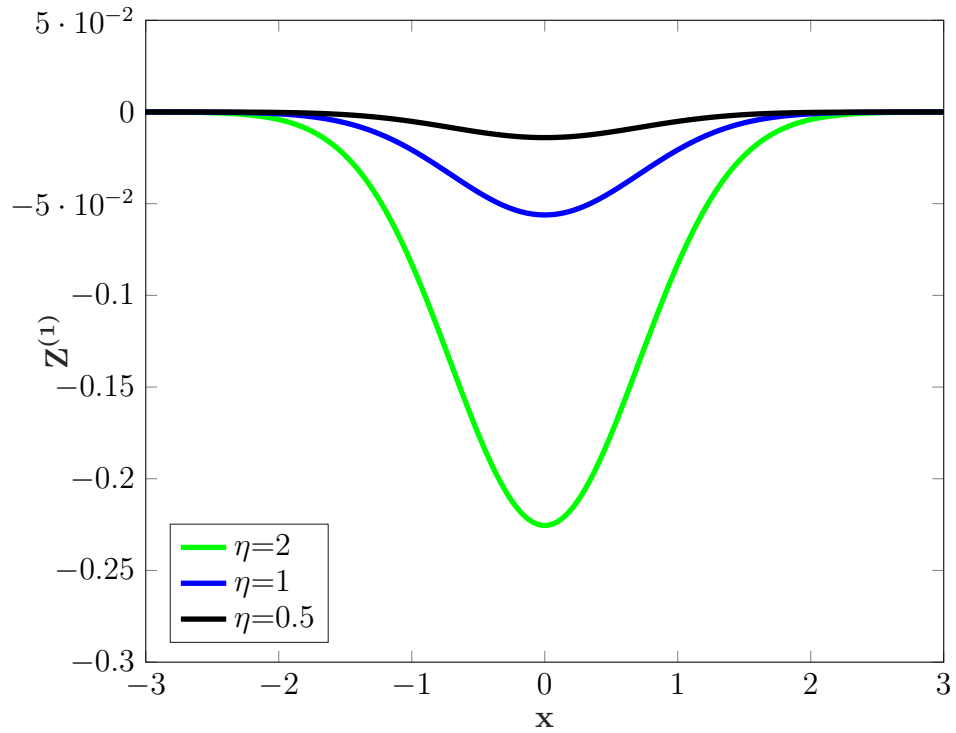


Figure 7.6: Variation of $\hat{Z}^{(1)}$ for $\mathcal{L}_F=1$, $\mathcal{L}_O=1$ and $\phi=1$

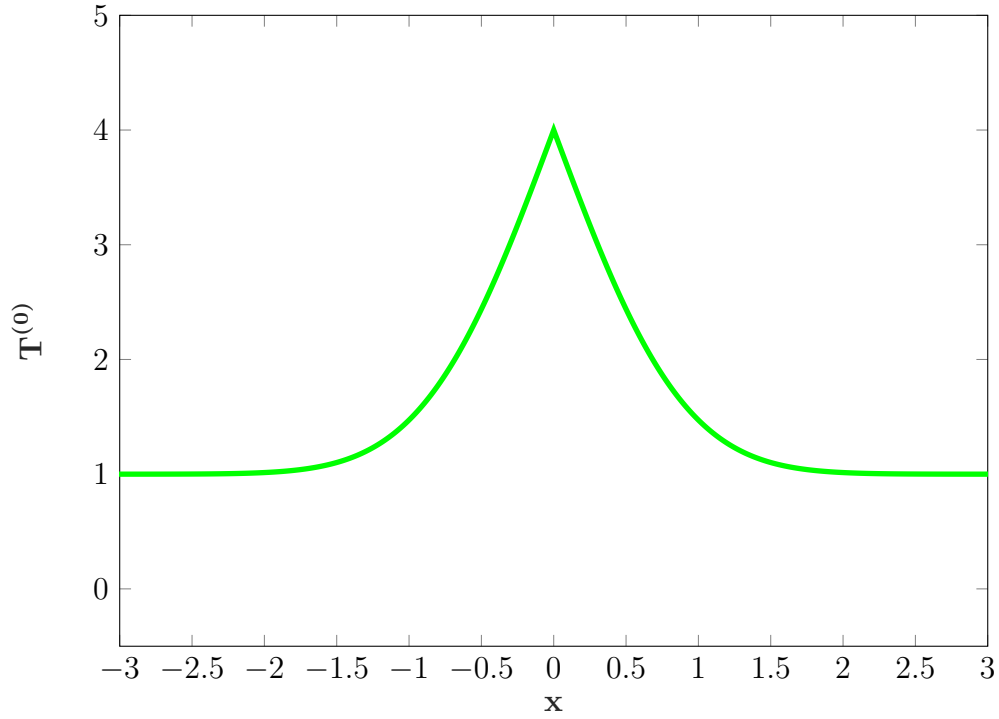


Figure 7.7: Variation of $T^{(0)}$ for $\mathcal{L}_F=1$, $\mathcal{L}_O=1$ and $\phi=1$

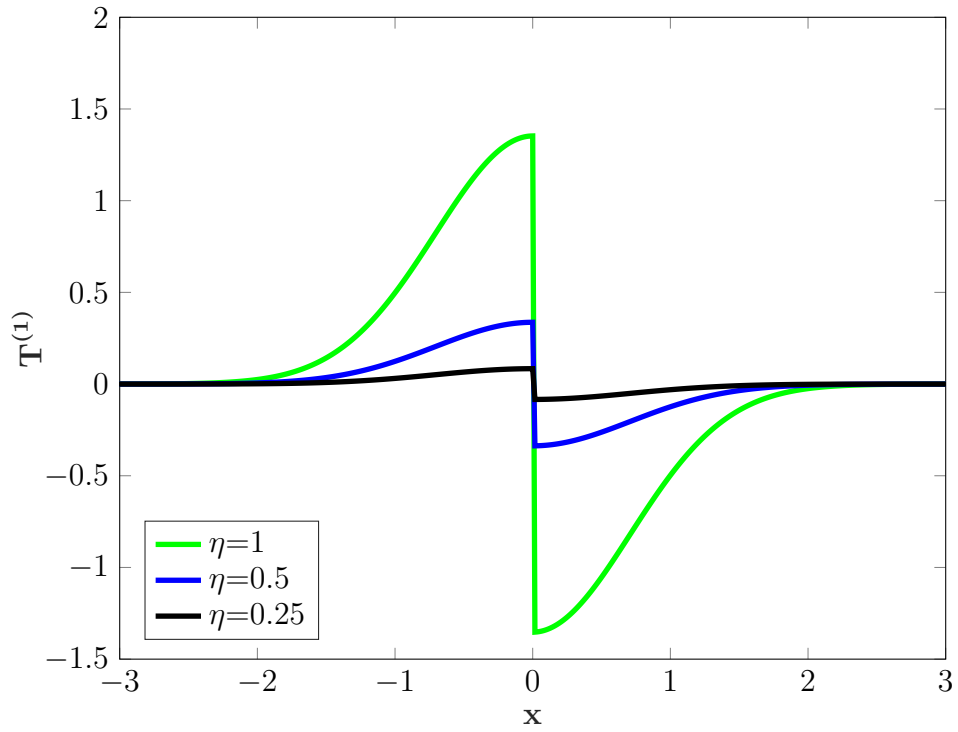


Figure 7.8: Variation of $T^{(1)}$ for $\mathcal{L}_F=1$, $\mathcal{L}_O=1$ and $\phi=1$

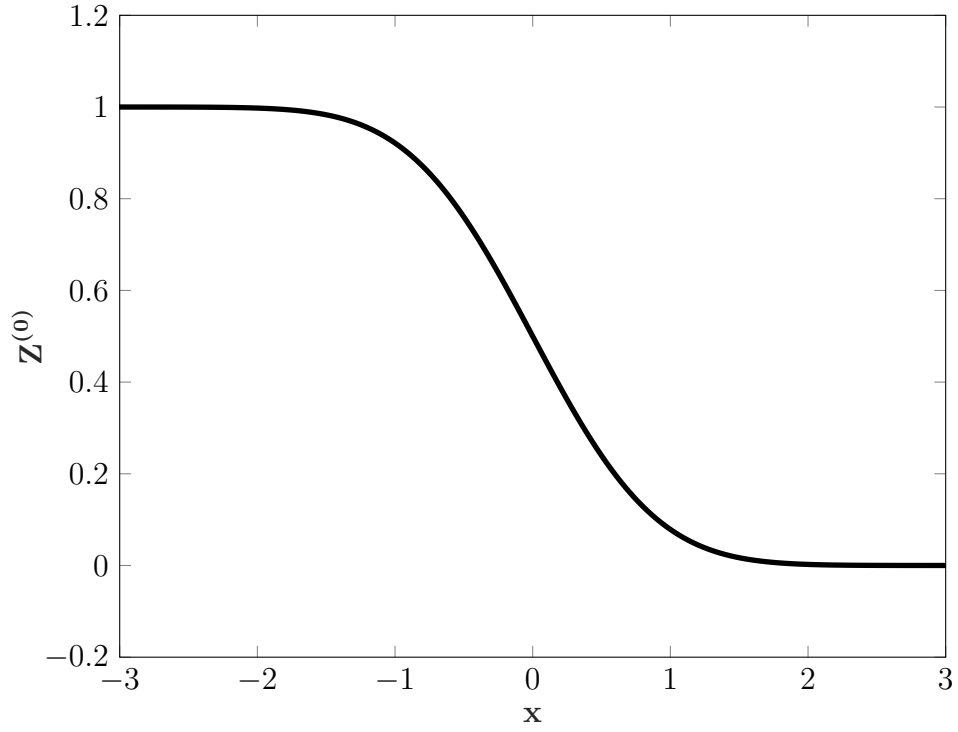


Figure 7.9: Variation of $\hat{Z}^{(0)}$ for $\mathcal{L}_F=1$, $\mathcal{L}_O=1$ and $\phi=2$

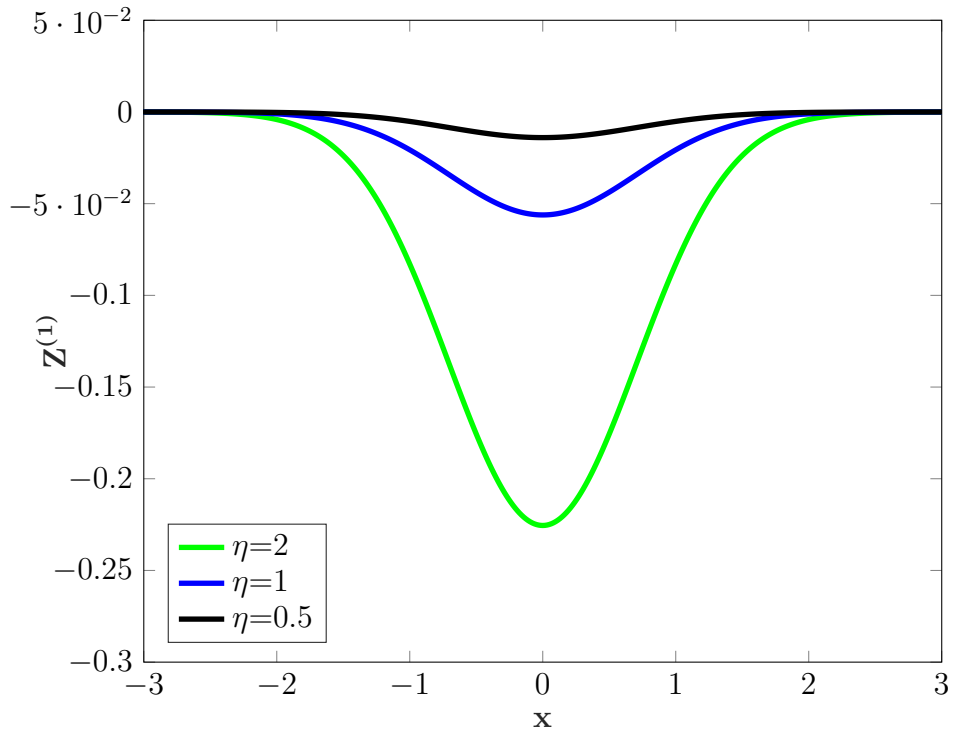


Figure 7.10: Variation of $\hat{Z}^{(1)}$ for $\mathcal{L}_F=1$, $\mathcal{L}_O=1$ and $\phi=2$

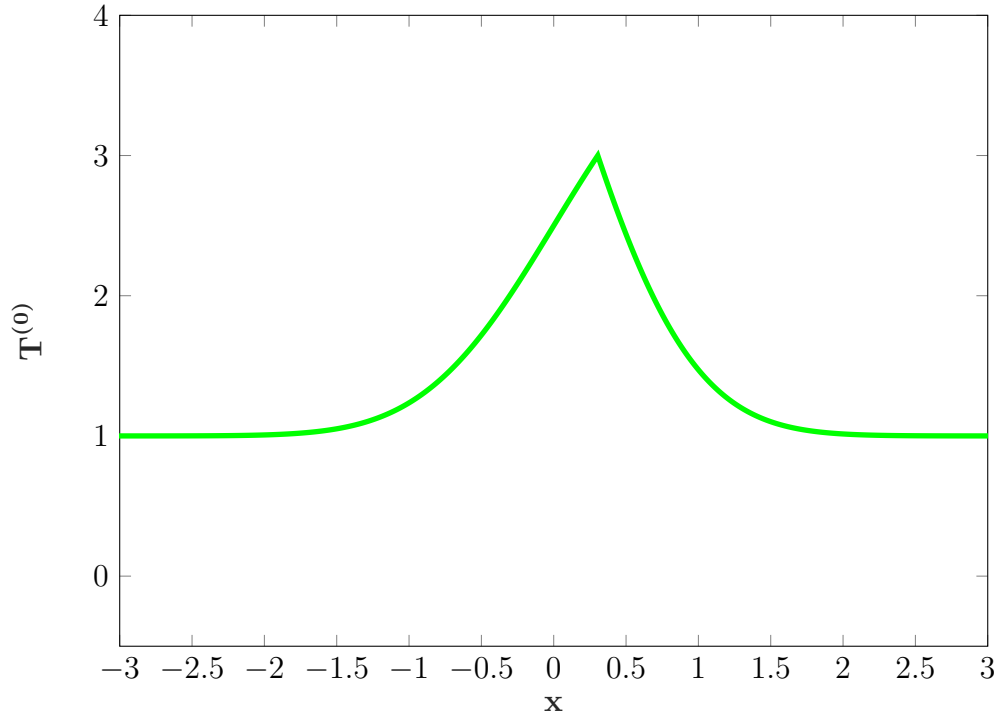


Figure 7.11: Variation of $T^{(0)}$ for $\mathcal{L}_F=1$, $\mathcal{L}_O=1$ and $\phi=2$

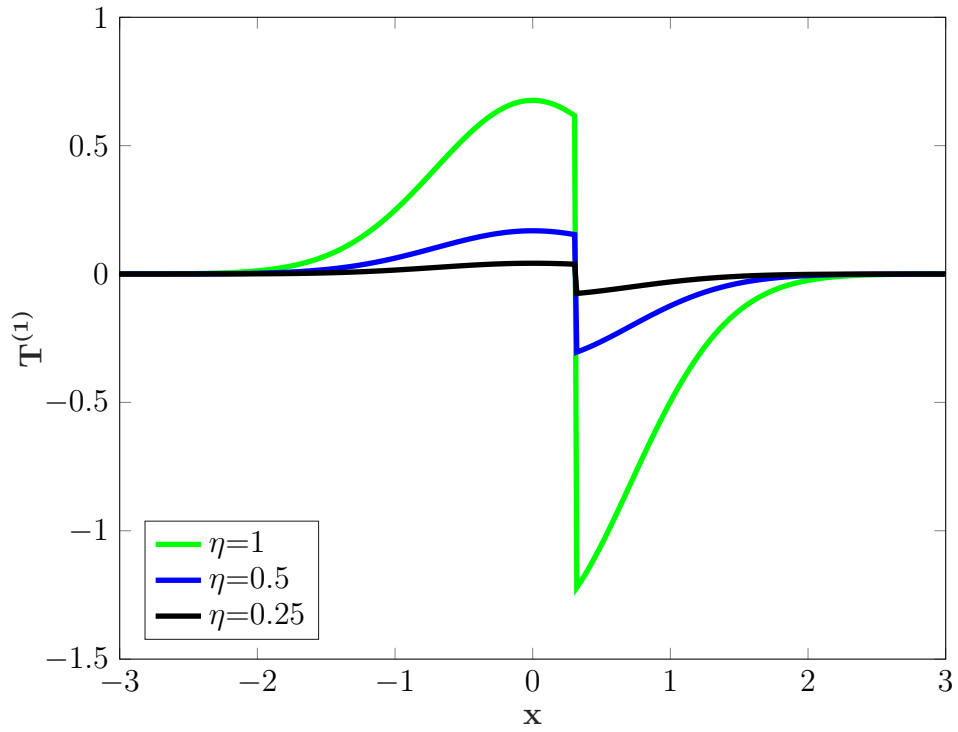


Figure 7.12: Variation of $T^{(1)}$ for $\mathcal{L}_F=1$, $\mathcal{L}_O=1$ and $\phi=2$

7.2 Unequal Lewis Numbers Case

In this section, the plots of $Z^{\hat{0}}$, $Z^{\hat{1}}$, $T^{(0)}$, and $T^{(1)}$ are presented for the combinations of \mathcal{L}_F , \mathcal{L}_O and ϕ given in Table 7.2.

\mathcal{L}_F	\mathcal{L}_O	ϕ	q	$x_f^{(0)}$
1.5	0.5	0.5	6	-0.611
1.5	0.5	1	6	-0.2616
1.5	0.5	2	6	0.0652

Table 7.2: Combinations of physical parameters considered for the unequal Lewis numbers case

Further, the dimensions of the domain considered are as follows:

Length of the domain along the x-direction, $L=16$.

Height of the domain along the η -direction, $W=2$.

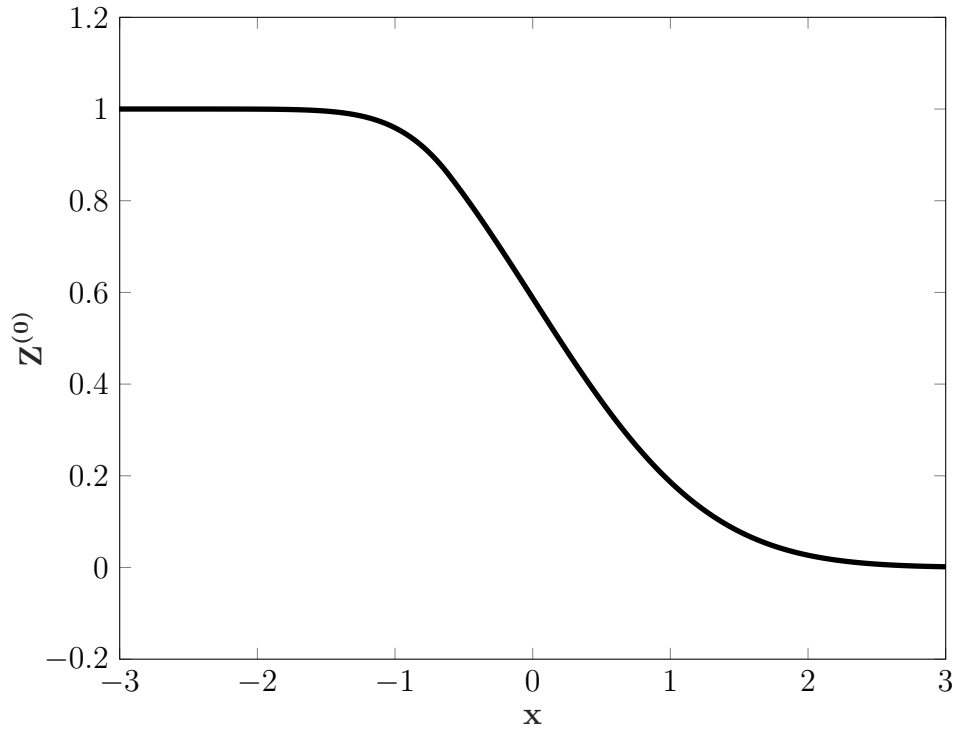


Figure 7.13: Variation of $\hat{Z}^{(0)}$ for $\mathcal{L}_F=1.5$, $\mathcal{L}_O=1.5$ and $\phi=0.5$

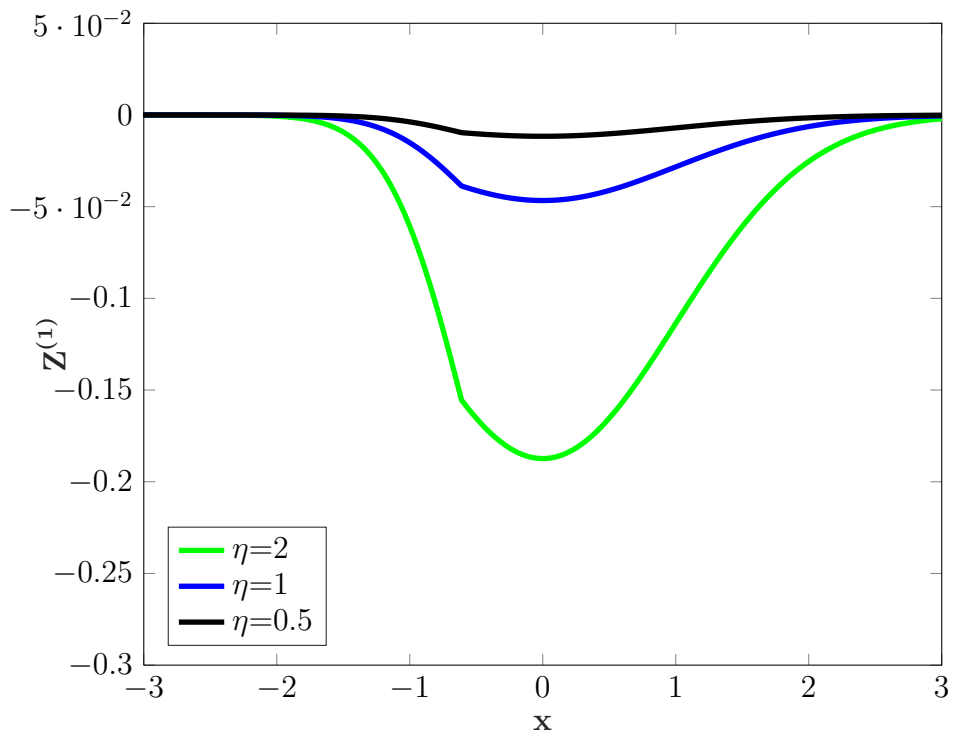


Figure 7.14: Variation of $\hat{Z}^{(1)}$ for $\mathcal{L}_F=1.5$, $\mathcal{L}_O=1.5$ and $\phi=0.5$

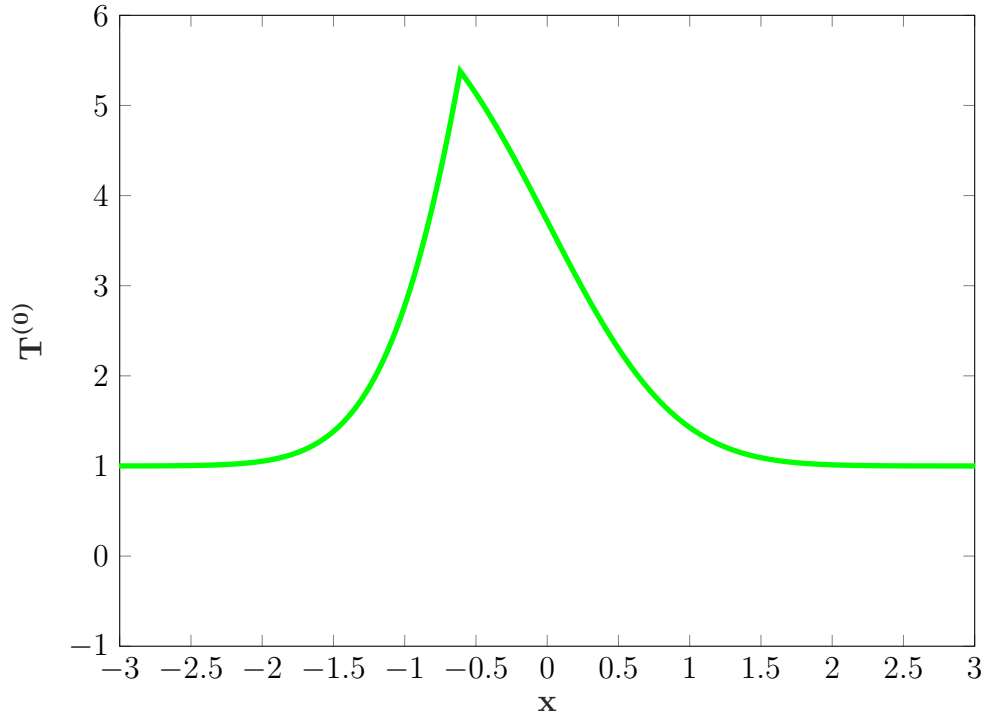


Figure 7.15: Variation of $T^{(0)}$ for $\mathcal{L}_F=1.5$, $\mathcal{L}_O=1.5$ and $\phi=0.5$

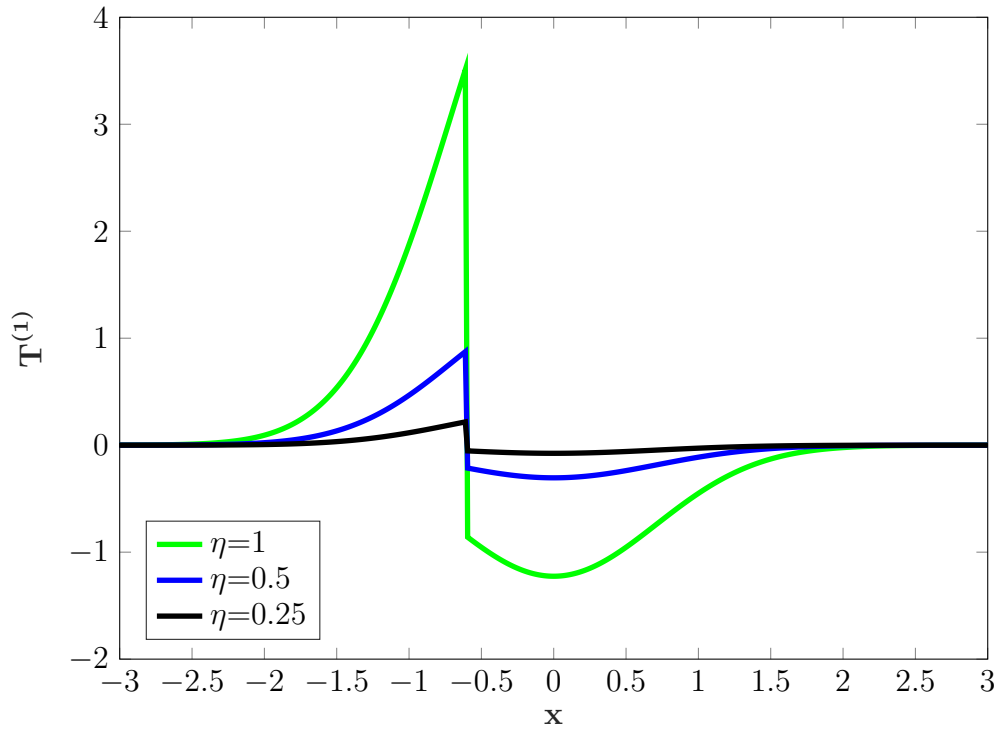


Figure 7.16: Variation of $T^{(1)}$ for $\mathcal{L}_F=1.5$, $\mathcal{L}_O=1.5$ and $\phi=0.5$

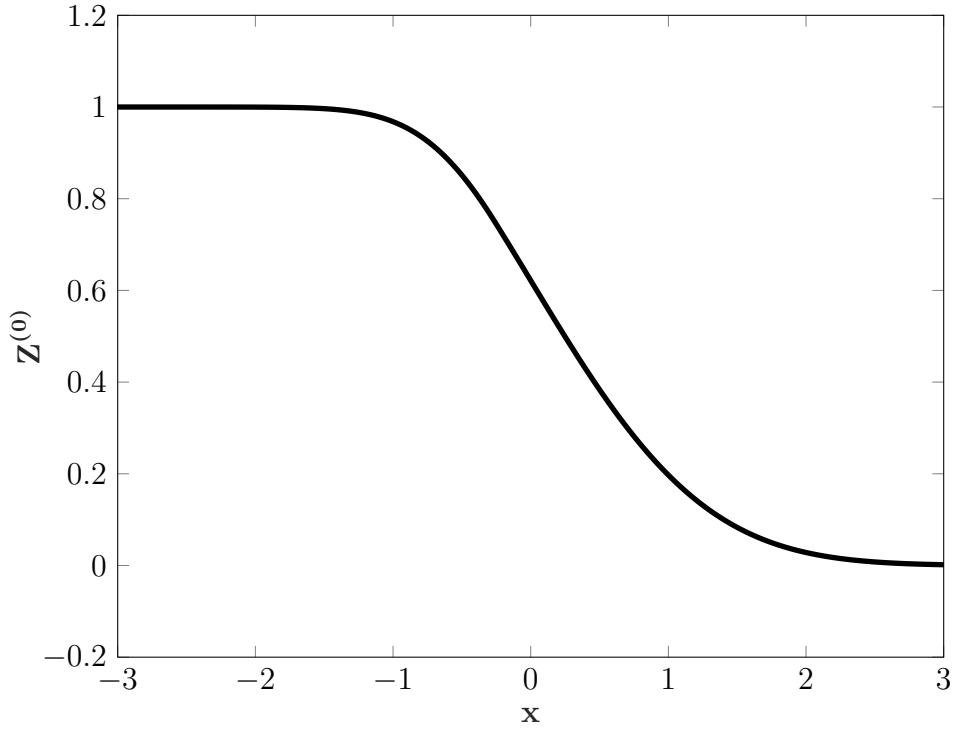


Figure 7.17: Variation of $\hat{Z}^{(0)}$ for $\mathcal{L}_F=1.5$, $\mathcal{L}_O=1.5$ and $\phi=1$

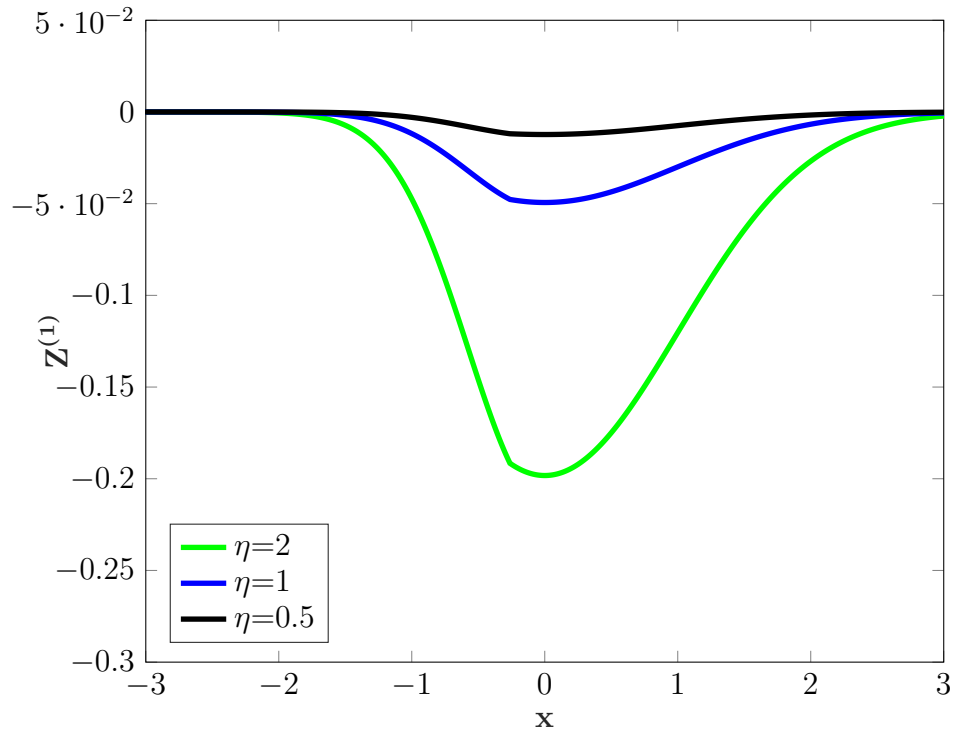


Figure 7.18: Variation of $\hat{Z}^{(1)}$ for $\mathcal{L}_F=1.5$, $\mathcal{L}_O=1.5$ and $\phi=1$

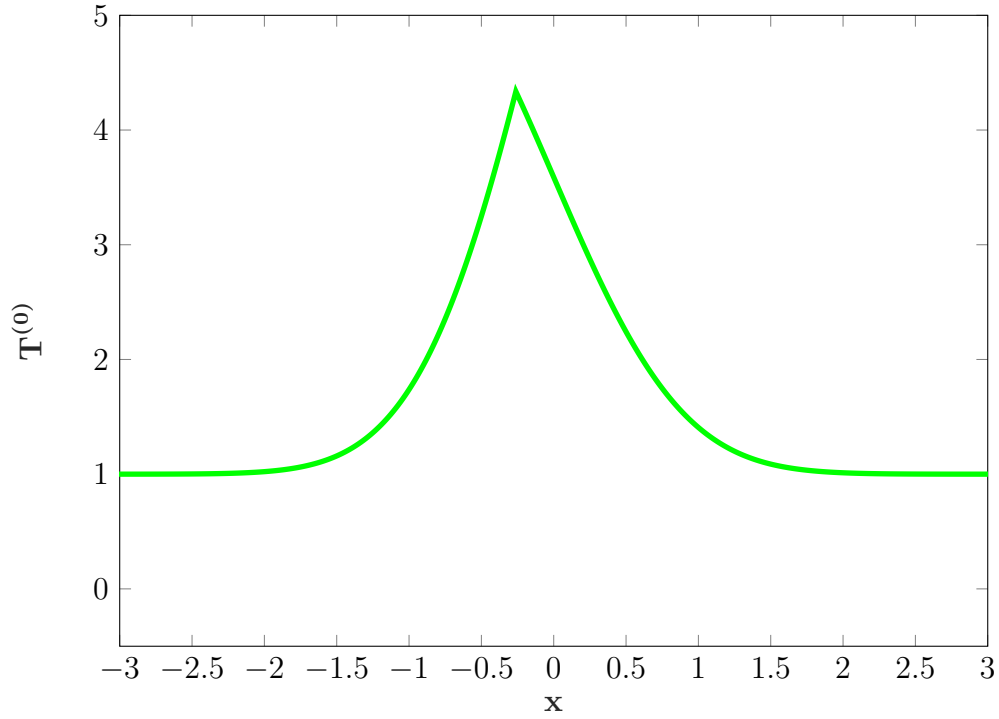


Figure 7.19: Variation of $T^{(0)}$ for $\mathcal{L}_F=1.5$, $\mathcal{L}_O=1.5$ and $\phi=1$

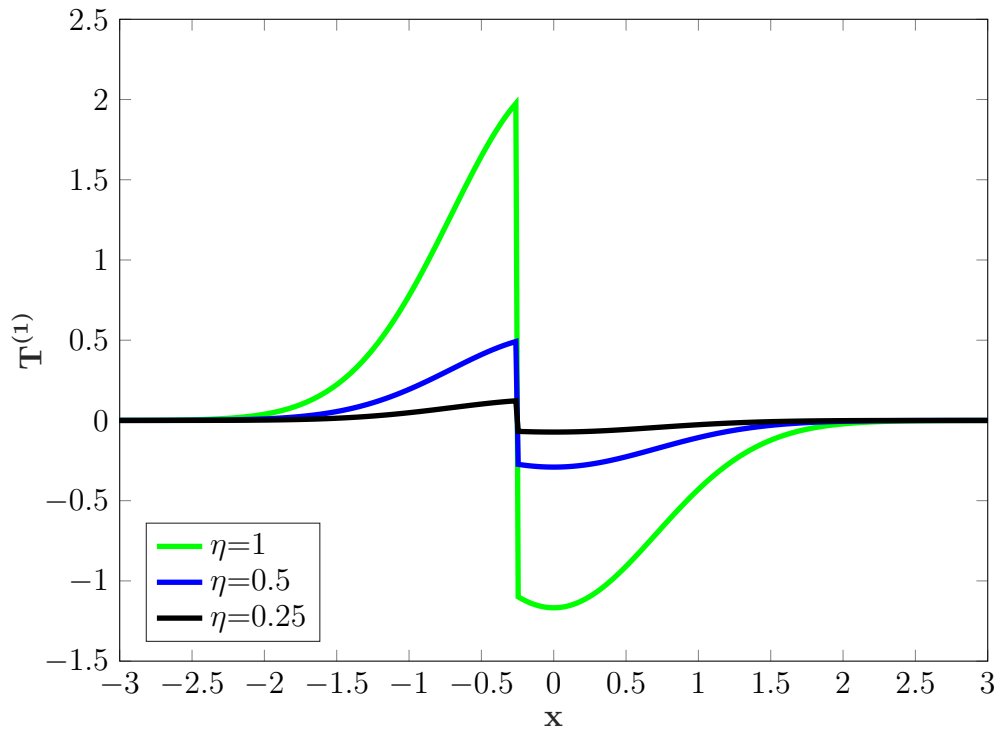


Figure 7.20: Variation of $T^{(1)}$ for $\mathcal{L}_F=1.5$, $\mathcal{L}_O=1.5$ and $\phi=1$

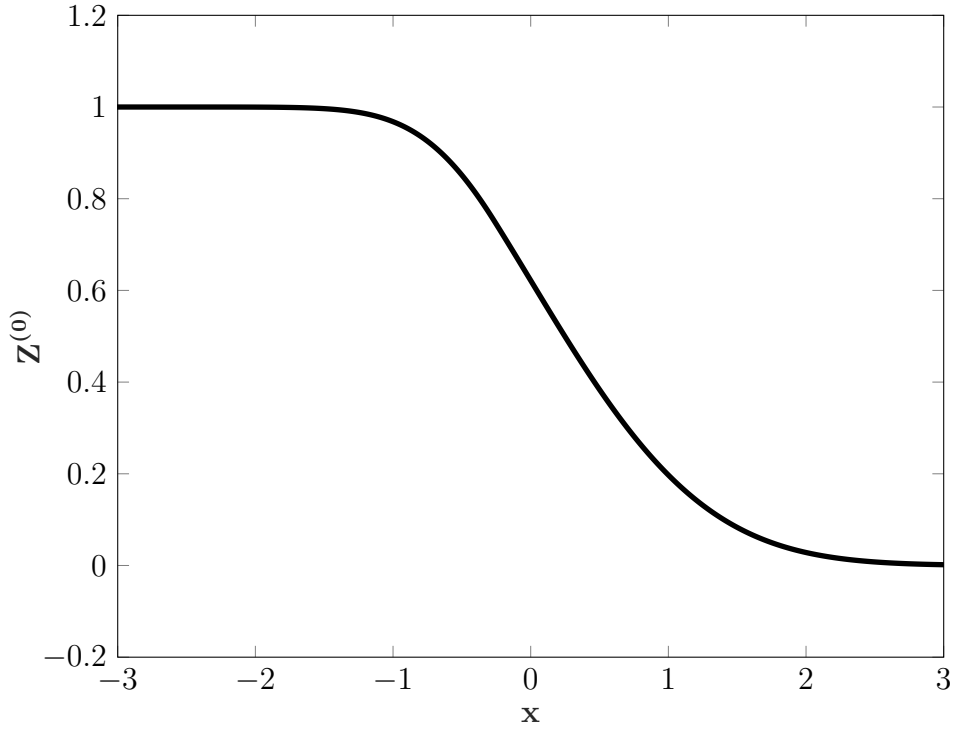


Figure 7.21: Variation of $\hat{Z}^{(0)}$ for $\mathcal{L}_F=1.5$, $\mathcal{L}_O=1.5$ and $\phi=2$

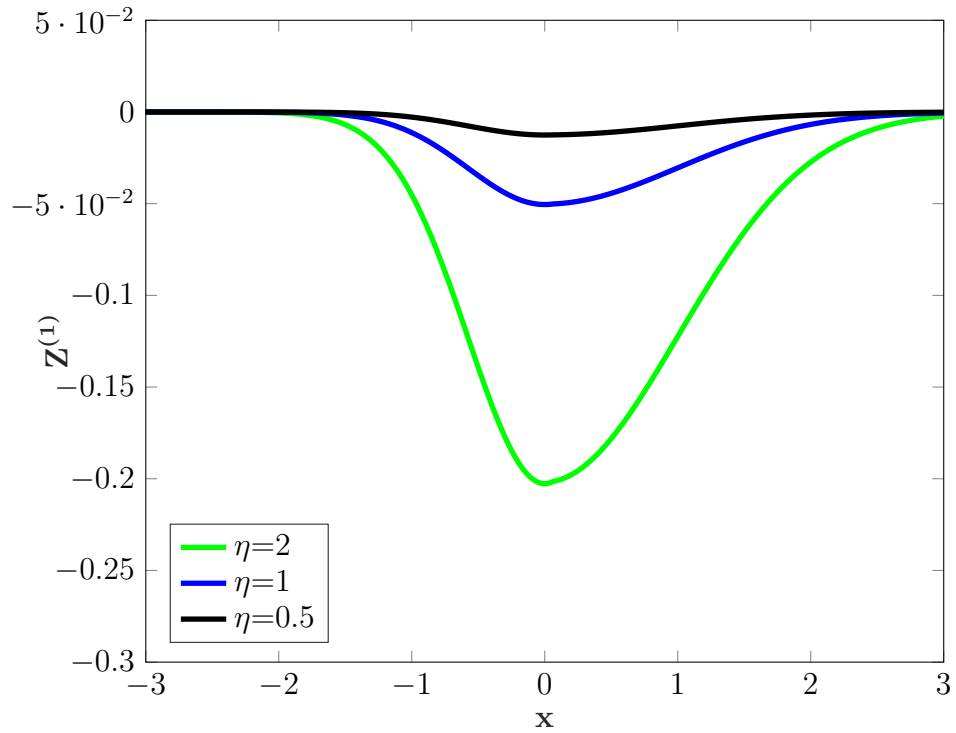


Figure 7.22: Variation of $\hat{Z}^{(1)}$ for $\mathcal{L}_F=1.5$, $\mathcal{L}_O=1.5$ and $\phi=2$

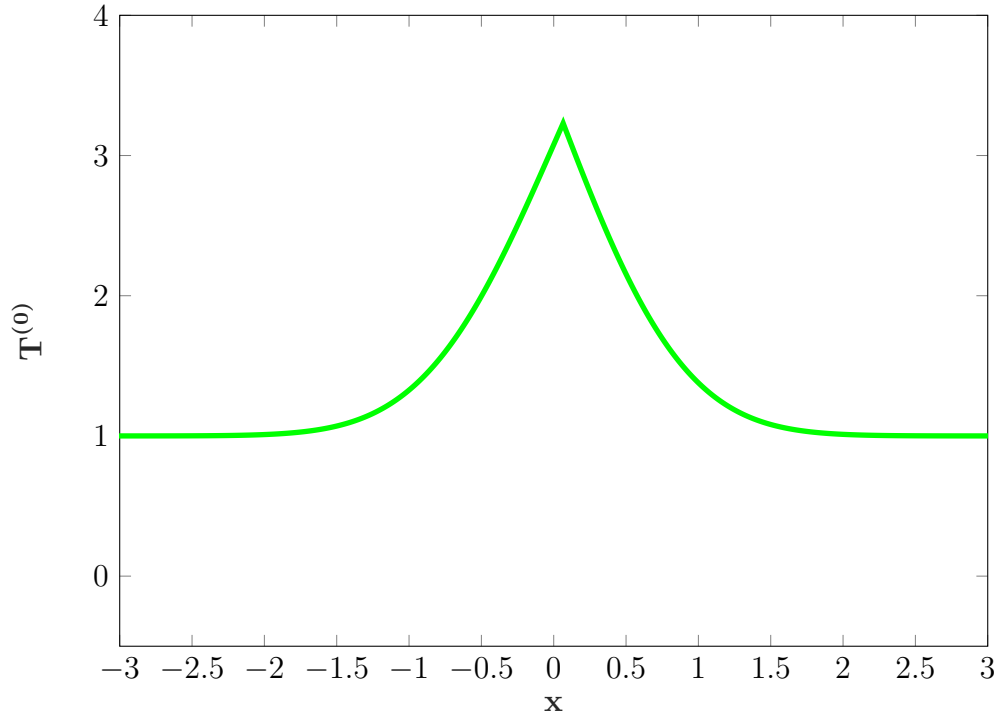


Figure 7.23: Variation of $T^{(0)}$ for $\mathcal{L}_F=1.5$, $\mathcal{L}_O=1.5$ and $\phi=2$

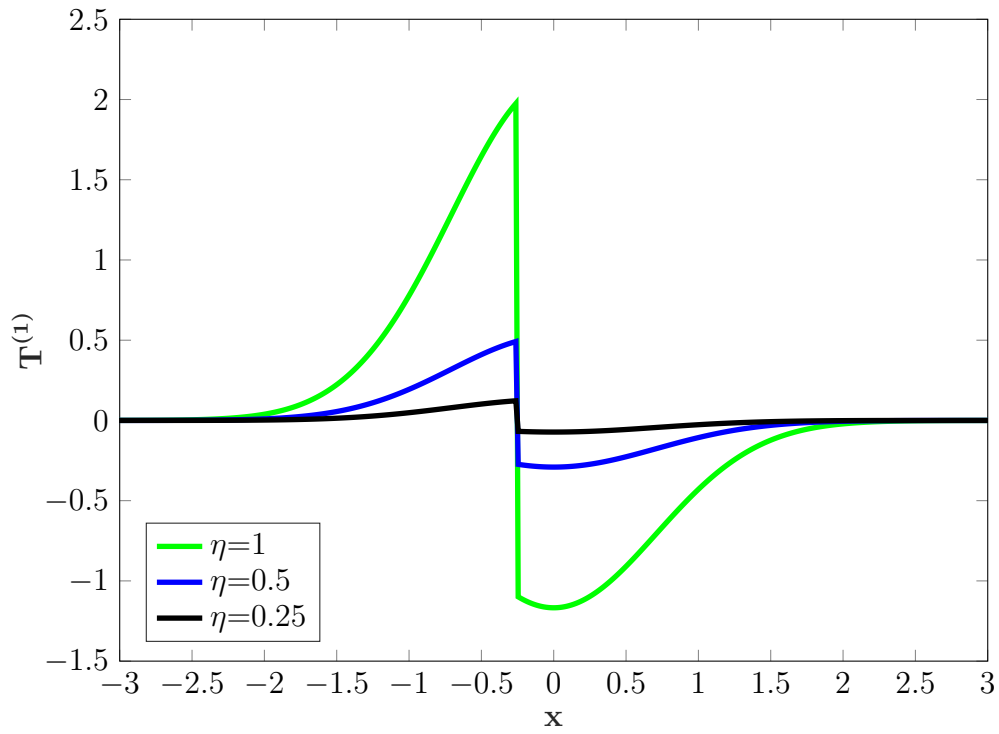


Figure 7.24: Variation of $T^{(1)}$ for $\mathcal{L}_F=1.5$, $\mathcal{L}_O=1.5$ and $\phi=2$

CHAPTER 8

CONCLUSIONS

To observe the fuel and oxidizer mass fraction distribution, shape, and temperature distribution along the reaction sheet of a counterflow diffusion flame system, we have built a steady, constant density based lower-order model. We have assumed the chemical activity to occur at an infinite rate and is confined to the reaction sheet. Further, we have also imposed a flow field comprising of a first order potential field which is superimposed upon a weak second order potential flow field. We have divided the analysis into two cases, the unity Lewis numbers case and the unequal Lewis numbers case. Using this model, we have shown the following:

- The reaction sheet always takes the shape of the separatrix, independent of the values of \mathcal{L}_F , \mathcal{L}_O , ϕ .
- Although the reaction sheet takes the exact shape of the separatrix, its position is determined by the values of \mathcal{L}_F , \mathcal{L}_O , and ϕ . This position is quantified by $x_f^{(0)}$.
- The temperature of the reaction sheet is constant for the unity Lewis numbers case and is called the ‘adiabatic temperature’, denoted by T_a . It is given by,

$$T_a = 1 + \frac{q}{1 + \phi}.$$

- It is also shown that for the unity Lewis number case at the Burke-Schumann limit and constant density, the temperature of the reaction sheet is always constant irrespective of the flow field.
- The temperature of the reaction sheet is constant for the unequal Lewis number case as well. This temperature is called the ‘stoichiometric

temperature', denoted by T_s . It is given by,

$$T_s = 1 + \frac{q}{2\sqrt{\mathcal{L}_F}} \exp\{(1 - \mathcal{L}_F)(x_f^{(0)})^2\} \frac{1 - \operatorname{erf}^2(x_f^{(0)})}{1 + \operatorname{erf}(\sqrt{\mathcal{L}_F}x_f^{(0)})}.$$

This shows that a first order correction to the flow field will not effect the stoichiometric temperature, at least to the first order.

REFERENCES

- SP Burke and TEW Schumann. Diffusion flames. *Industrial & Engineering Chemistry*, 20(10):998–1004, 1928.
- David R Kassoy and Forman A Williams. Effects of chemical kinetics on near equilibrium combustion in nonpremixed systems. *The Physics of Fluids*, 11(6):1343–1351, 1968.
- Zhilin Li and Kazufumi Ito. *The immersed interface method: numerical solutions of PDEs involving interfaces and irregular domains*. SIAM, 2006.

APPENDIX A

NUMERICAL METHODOLOGY TO SOLVE THE $\mathcal{O}(\epsilon)$ EQUATION FOR Z

The domain in which equation (4.16) is to be solved is shown in Figure A.1. It is defined as follows,

$$\begin{aligned} -W/2 &\leq x \leq W/2, \\ 0 &\leq \eta \leq L, \end{aligned}$$

where W and L are the lengths along the x and η directions respectively.

In equation (4.16), to eliminate the dependence of the stability of the solution on grid sizes in x and η directions, Δx and $\Delta \eta$ respectively, an implicit scheme was chosen. The domain is discretized as follows:

$$\begin{aligned} x_i &= -W/2 + \Delta x(i - 1), \quad i = 1 : N, \\ \eta_j &= \Delta \eta(j - 1), \quad j = 1 : M, \end{aligned}$$

where N and M are the number of x and η grid points respectively. As can be seen from equation (4.16), the governing equation is singular at $\eta = 0$. This necessitates the use of a semi-implicit integration scheme. A Crank-Nicolson scheme was chosen along the η direction while a centered scheme was chosen along the x direction. To avoid this singularity, equation (4.16) is discretized midway between any two grid points lying on the same vertical as shown in Figure (A.1).

From equation (4.16), we have,

$$\left(2x \frac{\partial Z^{(1)}}{\partial x} - 2\eta \frac{\partial Z^{(1)}}{\partial \eta} + \frac{1}{\mathcal{L}} \frac{\partial^2 Z^{(1)}}{\partial x^2} \right)_{i,j+\frac{1}{2}} = \left(-\sqrt{\frac{\mathcal{L}}{\pi}} \eta^2 e^{-x^2 \mathcal{L}} \right)_{i,j+\frac{1}{2}}. \quad (\text{A.1})$$

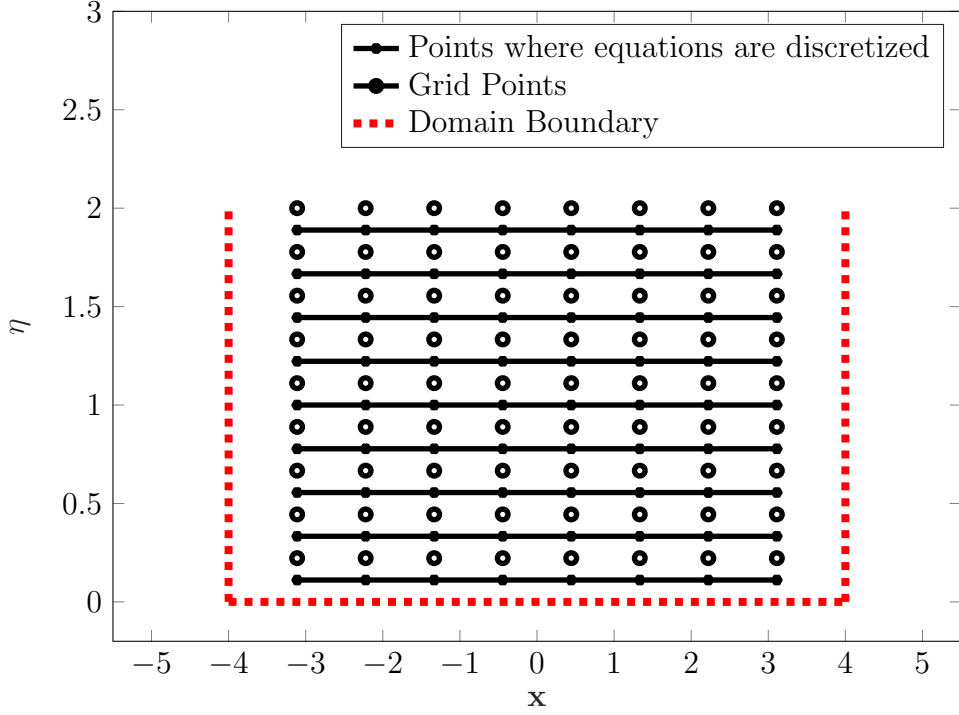


Figure A.1: Sample Computational Domain

The individual terms can be approximated as:

$$\begin{aligned} \left(2x \frac{\partial Z^{(1)}}{\partial x}\right)_{i,j+\frac{1}{2}} &= \frac{1}{2} \left\{ \left(2x \frac{\partial Z^{(1)}}{\partial x}\right)_{i,j+1} + \left(2x \frac{\partial Z^{(1)}}{\partial x}\right)_{i,j} \right\}, \\ \left(\frac{\partial Z^{(1)}}{\partial x}\right)_{i,j+\frac{1}{2}} &= \frac{1}{2} \left\{ \left(\frac{\partial^2 Z^{(1)}}{\partial x^2}\right)_{i,j+1} + \left(\frac{\partial^2 Z^{(1)}}{\partial x^2}\right)_{i,j} \right\}, \\ \left(-\sqrt{\frac{\mathcal{L}}{\pi}} \eta^2 e^{-x^2/\mathcal{L}}\right)_{i,j+\frac{1}{2}} &= -\sqrt{\frac{\mathcal{L}}{\pi}} \left(\frac{\eta_{j+1}^2 + \eta_j^2}{2}\right) e^{-x_i^2 \mathcal{L}}, \end{aligned}$$

hence,

$$\left(2x \frac{\partial Z^{(1)}}{\partial x}\right)_{i,j+1/2} = x_i \left(\frac{Z^{(1)}_{i+1,j} - Z^{(1)}_{i-1,j}}{2\Delta x} + \frac{Z^{(1)}_{i+1,j+1} - Z^{(1)}_{i-1,j+1}}{2\Delta x} \right), \quad (\text{A.2})$$

$$\left(2\eta \frac{\partial Z^{(1)}}{\partial \eta}\right)_{i,j+1/2} = (\eta_j + \eta_{j+1}) \frac{Z^{(1)}_{i,j+1} - Z^{(1)}_{i,j}}{\Delta \eta}, \quad (\text{A.3})$$

$$\left(\frac{\partial^2 Z^{(1)}}{\partial x^2}\right)_{i,j+1/2} = \frac{1}{2} \left(\frac{Z^{(1)}_{i+1,j+1} - 2Z^{(1)}_{i,j+1} + Z^{(1)}_{i-1,j+1}}{\Delta x^2} + \dots \right. \\ \left. \dots \frac{Z^{(1)}_{i+1,j} - 2Z^{(1)}_{i,j} + Z^{(1)}_{i-1,j}}{\Delta x^2} \right). \quad (\text{A.4})$$

Substituting equations (A.2)-(A.4) into equation (4.16) and by applying the boundary conditions (4.11)-(4.14), (4.16) can be solved. To confirm the correctness of the method, we look at the results of a grid-dependency test. Since the equation we are solving is parabolic, we define an L^1 norm to estimate the error, $\|e\|_1$. It is defined as,

$$\|e\|_1 = \sum_{i=1}^{N_0} \sum_{j=1}^{N_0} |Z_{ref}^{(1)}(x_i, \eta_j) - Z_N^{(1)}(x_i, \eta_j)| \Delta \eta \Delta x,$$

where N_0 is the number of grid points in both the x and η directions corresponding to the test case Z_{1N} . Z_{1ref} corresponds to the analytical solution (4.24). The results of the grid dependency studies shows that the value of $Z^{(1)}$ approaches the analytical solution with a second order convergence. This validates the use of the scheme and the correctness of the analytical solution.

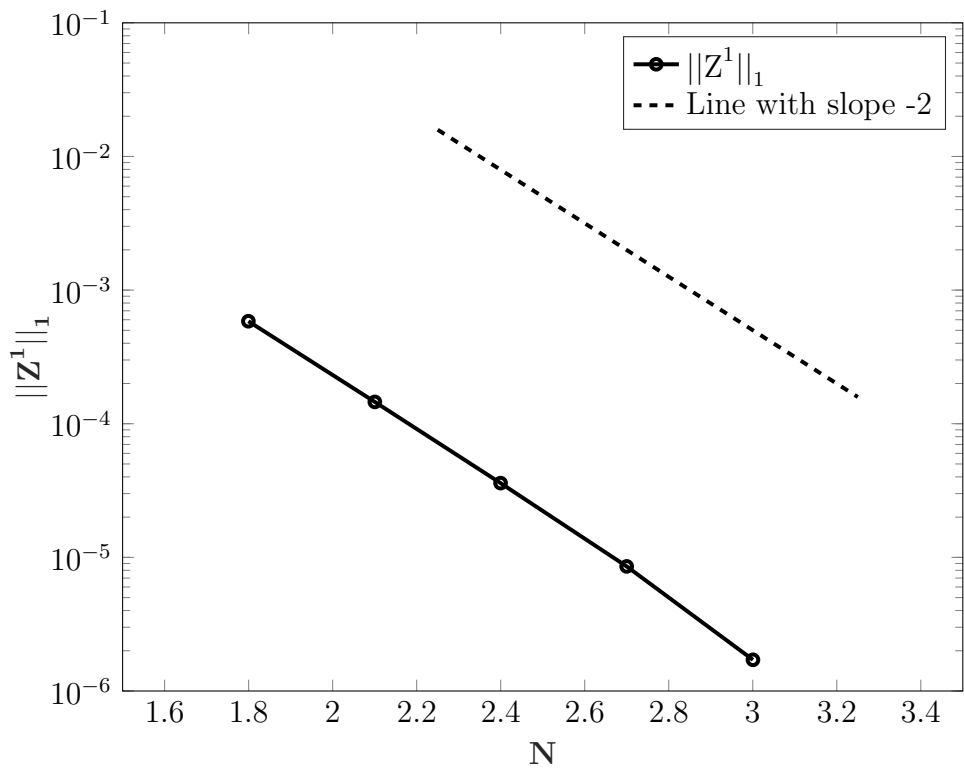


Figure A.2: Results of Grid Dependency Studies

APPENDIX B

NUMERICAL METHODOLOGY TO SOLVE FOR $\mathcal{O}(\epsilon)$ COMPONENT OF \hat{Z}

Unlike $Z^{(1)}$, solving for $\hat{Z}^{(1)}$ requires the consideration of the jump conditions given in equations (5.18) and (5.26). It is to be noted that since the jump conditions for $\hat{Z}^{(1)}$ depend on χ which also depends on $\hat{Z}^{(1)}$ through equation (5.27), the equation to be solved for $\hat{Z}^{(1)}$ is implicit in nature. Therefore, we use the following algorithm :

1. Since we have ascertained at (5.31) that χ is a second order monomial in η , i.e, $\chi = k\eta^2$, we make the initial guesses on k to be equal to $k = 1$ and $k = 2$.
2. With both the values of k chosen, we have the value of the boundary condition at $x = x_f^{(0)}$ using (5.14).
3. With the boundary condition at $x = x_f^{(0)}$ and using the boundary conditions (4.12), we can solve for (5.11) for both the values of k .
4. Using the values of $\hat{Z}^{(1)}$ thus obtained for each k , define a correction function, $\theta(k)$, as

$$\theta(k) = \left[\left[\frac{\partial \hat{Z}^{(1)}}{\partial x} \right] \right]_{x_f^{(0)}} + \chi \left[\left[\frac{d^2 \hat{Z}^{(0)}}{dx^2} \right] \right]_{x_f^{(0)}}. \quad (\text{B.1})$$

5. Find the value of k for which the jump condition is (5.26) satisfied, i.e, $\theta(k) = 0$ by linear interpolation.
6. Replace one of the initial guesses with the value of the new k obtained in the step above and iterate steps (1) to (5) till the two values of k are close enough to each other. In this excersice, a iteration was carried till the values of k fell within a range of 10^{-8} of each other.

APPENDIX C

NUMERICAL METHODOLOGY TO SOLVE FOR $T^{(1)}$

C.1 Numerical Methodology

The equation (6.4) is parabolic in nature. Since there is no analytical solution, the equation has to be solved numerically. If solved explicitly, the presence of a diffusion term makes it harder to get larger step sizes in η . This necessitates the need for a semi-implicit scheme. Crank-Nicolson is chosen. The domain is defined as follows

$$x_i = -W/2 + \Delta x(i - 1), i = 1 : N,$$
$$\eta_j = \Delta \eta(j - 1), j = 1 : M,$$

where N and M are the number of x and η grid points respectively. The domain is discretized in such a way that the vertical $x = x_f^{(0)}$ lies on a grid point. Let us call the address of this point as I . The arrangement of the grid points is as shown in the figure (C.1).

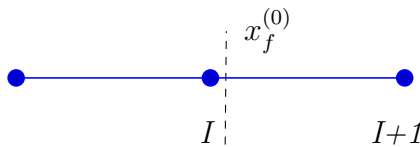


Figure C.1: Arrangement of the grid points about the position $x_f^{(0)}$

Since the equation (6.4) is singular at $\eta = 0$. To avoid this singularity, equation (6.4) is discretized midway between any two grid points lying on the same vertical as shown in Figure (A.1).

For any point, x_i in the domain satisfying the condition $x < x_I$ and

$x > x_{I+1}$, equation (3.22) can be discretized as follows,

$$\left(2x \frac{\partial T^{(1)}}{\partial x} - 2\eta \frac{\partial T^{(1)}}{\partial \eta} + \frac{\partial^2 T^{(1)}}{\partial x^2}\right)_{i,j+\frac{1}{2}} = \left(-\eta^2 \frac{dT^{(0)}}{dx}\right)_{i,j+\frac{1}{2}}. \quad (\text{C.1})$$

The individual terms can be approximated as:

$$\begin{aligned} \left(2x \frac{\partial T^{(1)}}{\partial x}\right)_{i,j+\frac{1}{2}} &= \frac{1}{2} \left\{ \left(2x \frac{\partial T^{(1)}}{\partial x}\right)_{i,j+1} + \left(2x \frac{\partial T^{(1)}}{\partial x}\right)_{i,j} \right\}, \\ \left(\frac{\partial T^{(1)}}{\partial x}\right)_{i,j+\frac{1}{2}} &= \frac{1}{2} \left\{ \left(\frac{\partial^2 T^{(1)}}{\partial x^2}\right)_{i,j+1} + \left(\frac{\partial^2 T^{(1)}}{\partial x^2}\right)_{i,j} \right\}, \\ \left(\eta^2 \frac{dT^{(0)}}{dx}\right)_{i,j+\frac{1}{2}} &= \left(\frac{\eta_{j+1}^2 + \eta_j^2}{2}\right) \frac{dT^{(0)}}{dx} \Big|_i, \end{aligned}$$

hence,

$$\left(2x \frac{\partial T^{(1)}}{\partial x}\right)_{i,j+1/2} = x_i \left(\frac{T^{(1)}_{i+1,j} - T^{(1)}_{i-1,j}}{2\Delta x} + \frac{T^{(1)}_{i+1,j+1} - T^{(1)}_{i-1,j+1}}{2\Delta x} \right), \quad (\text{C.2})$$

$$\left(2\eta \frac{\partial T^{(1)}}{\partial \eta}\right)_{i,j+1/2} = (\eta_j + \eta_{j+1}) \frac{T^{(1)}_{i,j+1} - T^{(1)}_{i,j}}{\Delta \eta}, \quad (\text{C.3})$$

$$\begin{aligned} \left(\frac{\partial^2 T^{(1)}}{\partial x^2}\right)_{i,j+1/2} &= \frac{1}{2} \left(\frac{T^{(1)}_{i+1,j+1} - 2T^{(1)}_{i,j+1} + T^{(1)}_{i-1,j+1}}{\Delta x^2} + \dots \right. \\ &\quad \left. \dots + \frac{T^{(1)}_{i+1,j} - 2T^{(1)}_{i,j} + T^{(1)}_{i-1,j}}{\Delta x^2} \right). \end{aligned} \quad (\text{C.4})$$

But, the points corresponding to I and $I + 1$ cannot be approximated in the way mentioned above because of the presence of jumps in $T^{(1)}$ across the reaction sheet. Since we have jumps or discontinuities in $T^{(1)}$ and $\frac{\partial T^{(1)}}{\partial x}$, we have to use the Immersed Interface Method which will be discussed in the next section.

C.2 Immersed Interface Method

From (C.1), at $x = x_{f-}^{(0)}$ we have,

$$\begin{aligned}
& x_f^{(0)} \left(\frac{\partial T^{(1)}}{\partial x} \Big|_{x_{f-}^{(0),j}} + \frac{\partial T^{(1)}}{\partial x} \Big|_{x_{f-}^{(0),j+1}} \right) - (\eta_j + \eta_{j+1}) \frac{\partial T^{(1)}}{\partial \eta} \Big|_{x_{f-}^{(0),j+\frac{1}{2}}} + \dots \\
& \dots + \frac{1}{2} \left(\frac{\partial^2 T^{(1)}}{\partial x^2} \Big|_{x_{f-}^{(0),j+1}} + \frac{\partial^2 T^{(1)}}{\partial x^2} \Big|_{x_{f-}^{(0),j}} \right) = -(\eta_{j+1}^2 + \eta_j^2) \frac{dT^0}{dx} \Big|_{x_{f-}^{(0)}}, \\
\Rightarrow & \frac{\partial T^{(1)}}{\partial \eta} \Big|_{x_{f-}^{(0),j+\frac{1}{2}}} - \left[\frac{x_f^{(0)}}{\eta_j + \eta_{j+1}} \frac{\partial T^{(1)}}{\partial x} \Big|_{x_{f-}^{(0),j}} + \frac{x_f^{(0)}}{\eta_j + \eta_{j+1}} \frac{\partial T^{(1)}}{\partial x} \Big|_{x_{f+}^{(0),j+1}} + \dots \right. \\
& \dots + \frac{1}{2(\eta_j + \eta_{j+1})} \frac{\partial^2 T^{(1)}}{\partial x^2} \Big|_{x_{f-}^{(0),j+1}}, \left. + \frac{1}{2(\eta_j + \eta_{j+1})} \frac{\partial^2 T^{(1)}}{\partial x^2} \Big|_{x_{f-}^{(0),j}} + \dots \right. \\
& \left. \dots + \frac{(\eta_{j+1}^2 + \eta_j^2)}{\eta_{j+1} + \eta_j} \frac{dT^0}{dx} \Big|_{x_{f-}^{(0)}} \right] = 0.
\end{aligned} \tag{C.5}$$

With this mind, we approximate the $\mathcal{O}(\epsilon)$ equation at I assuming the generic form given below. The coefficients are determined using the method of undetermined coefficients.

$$\begin{aligned}
\frac{T_{I,j+1}^{(1)} - T_{I,j}^{(1)}}{\Delta \eta} = \frac{1}{2} \left\{ a_1^1 T_{I+1,j+1}^{(1)} + a_2^1 T_{I,j+1}^{(1)} + a_3^1 T_{I-1,j+1}^{(1)} + a_1 T_{I+1,j}^{(1)} + \dots \right. \\
\left. \dots + a_2 T_{I,j}^{(1)} + a_3 T_{I-1,j}^{(1)} - f_{I,j+1} - f_{I,j} - C_{I,j} - C_{I,j+1} \right\}
\end{aligned} \tag{C.6}$$

where a_k, a_k^1 ($k = 1, 2, 3$) are the coefficients to be determined. $C_{I,j+1}, C_{I,j}$ are called the correction terms and $f_{I,j+1}, f_{I,j}$ are source terms. The truncation error, τ , in the above equation is given by,

$$\begin{aligned}
\tau = \frac{T_{I,j+1}^{(1)} - T_{I,j}^{(1)}}{\Delta \eta} - \frac{1}{2} \left\{ a_1^1 T_{I+1,j+1}^{(1)} + a_2^1 T_{I,j+1}^{(1)} + a_3^1 T_{I-1,j+1}^{(1)} + \dots \right. \\
\left. \dots + a_1 T_{I+1,j}^{(1)} + a_2 T_{I,j}^{(1)} + a_3 T_{I-1,j}^{(1)} - f_{I,j+1} - f_{I,j} - C_{I,j} - C_{I,j+1} \right\}
\end{aligned} \tag{C.7}$$

Using Taylor expansion for $T_{I+1,j+1}^{(1)}$, we have

$$\begin{aligned} T_{I+1,j+1}^{(1)} &= T_{x_{f+}^{(0)},j+1}^{(1)} + (x_{I+1} - x_f^{(0)}) \frac{\partial T^{(1)}}{\partial x} \Big|_{x_{f+}^{(0)},j+1} + \dots \\ &\dots + \frac{(x_{j+1} - x_f^{(0)})^2}{2} \frac{\partial^2 T^{(1)}}{\partial x^2} \Big|_{x_{f+}^{(0)},j+1} + \mathcal{O}(\Delta x^3). \end{aligned}$$

Using the jump relations, the above equation can be written as

$$\begin{aligned} T_{I+1,j+1}^{(1)} &= T_{x_{f-}^{(0)},j+1}^{(1)} + \llbracket T^{(1)} \rrbracket_{x_{f-}^{(0)},j+1} + \dots \\ &\dots + (x_{I+1} - x_f^{(0)}) \left(\llbracket \frac{\partial T^{(1)}}{\partial x} \rrbracket_{x_{f-}^{(0)},j+1} + \frac{\partial T^{(1)}}{\partial x} \Big|_{x_{f-}^{(0)},j+1} \right) + \dots \quad (\text{C.8}) \\ &\dots + \frac{(x_{I+1} - x_f^{(0)})^2}{2} \left(\frac{\partial T^{(1)}}{\partial x} \Big|_{x_{f-}^{(0)},j+1} + \llbracket \frac{\partial^2 T^{(1)}}{\partial x^2} \rrbracket_{x_{f-}^{(0)},j+1} \right) + \mathcal{O}(\Delta x^3). \end{aligned}$$

From (C.1), at $x = x_{f+}^{(0)}$ and $x = x_{f-}^{(0)}$, we have,

$$2x_f^{(0)} \frac{\partial T^{(1)}}{\partial x} \Big|_{x_{f+}^{(0)},j} - 2\eta \frac{\partial T^{(1)}}{\partial \eta} \Big|_{x_{f+}^{(0)},j} + \frac{\partial^2 T^{(1)}}{\partial x^2} \Big|_{x_{f+}^{(0)},j} = -\eta^2 \frac{dT^0}{dx} \Big|_{x_{f+}^{(0)},j} \quad (\text{C.9})$$

and

$$2x_f^{(0)} \frac{\partial T^{(1)}}{\partial x} \Big|_{x_{f-}^{(0)},j} - 2\eta \frac{\partial T^{(1)}}{\partial \eta} \Big|_{x_{f-}^{(0)},j} + \frac{\partial^2 T^{(1)}}{\partial x^2} \Big|_{x_{f-}^{(0)},j} = -\eta^2 \frac{dT^0}{dx} \Big|_{x_{f-}^{(0)},j} \quad (\text{C.10})$$

respectively. Subtracting (C.10) and (C.9),

$$2x_f^{(0)} \llbracket \frac{\partial T^{(1)}}{\partial x} \rrbracket_{x_f^{(0)},j} - 2\eta \llbracket \frac{\partial T^{(1)}}{\partial \eta} \rrbracket_{x_f^{(0)},j} + \llbracket \frac{\partial^2 T^{(1)}}{\partial x^2} \rrbracket_{x_f^{(0)},j} + \eta^2 \llbracket \frac{dT^0}{dx} \rrbracket_{x_f^{(0)},j} = 0$$

$$\implies \left[\left[\frac{\partial^2 T^{(1)}}{\partial x^2} \right] \right]_{x_f^{(0)},j} = -\eta^2 \left[\left[\frac{dT^{(0)}}{dx} \right] \right]_{x_f^{(0)},j} + 2x_f^{(0)} \left[\left[\frac{\partial T^{(1)}}{\partial x} \right] \right]_{x_f^{(0)},j} - 2\eta \left[\left[\frac{\partial T^{(1)}}{\partial \eta} \right] \right]_{x_f^{(0)},j}. \quad (\text{C.11})$$

Now,

$$\begin{aligned} \left[\left[\frac{\partial T^{(1)}}{\partial \eta} \right] \right]_{x_f^{(0)},j} &= \left. \frac{\partial T^{(1)}}{\partial \eta} \right|_{x_{f+}^{(0)},j} - \left. \frac{\partial T^{(1)}}{\partial \eta} \right|_{x_{f-}^{(0)},j} = \\ &= \frac{\partial}{\partial \eta} \left(T^{(1)} \Big|_{x_{f+}^{(0)},j} - T^{(1)} \Big|_{x_{f-}^{(0)},j} \right) = \frac{\partial}{\partial \eta} \left[T^{(1)} \right]_{x_f^{(0)},j} \end{aligned} \quad (\text{C.12})$$

Using (6.12),

$$\frac{\partial}{\partial \eta} \left[T^{(1)} \right]_{x_f^{(0)},j} = -\frac{\partial}{\partial \eta} \left[\chi \frac{dT^{(0)}}{dx} \right]_{x_f^{(0)}} = -\frac{\partial \chi}{\partial \eta} \left[\frac{dT^{(0)}}{dx} \right]_{x_f^{(0)}} \quad (\text{C.13})$$

Using (5.27),

$$\frac{\partial \chi}{\partial \eta} = -\left. \frac{\partial \hat{Z}^{(1)}}{\partial \eta} \right|_{x_f^{(0)},\eta_j} \left(\frac{d\hat{Z}^{(0)}(x_f^{(0)})}{dx} \right)^{-1}. \quad (\text{C.14})$$

Using (C.13), (C.14) in (C.11),

$$\begin{aligned} \left[\left[\frac{\partial^2 T^{(1)}}{\partial x^2} \right] \right]_{x_f^{(0)},j} &= -\eta_j^2 \left[\left[\frac{dT^{(0)}}{dx} \right] \right]_{x_f^{(0)},j} + 2x_f^{(0)} \left[\left[\frac{\partial T^{(1)}}{\partial x} \right] \right]_{x_f^{(0)},j} + \dots \\ &\dots + \left\{ 2\eta_j \left. \frac{\partial Z^1}{\partial \eta} \right|_{x_f^{(0)},\eta_j} \left[\left[\frac{dT^{(0)}}{dx} \right] \right]_{x_f^{(0)}} \left(\frac{dZ_0(x_f^{(0)})}{dx} \right)^{-1} \right\}. \end{aligned} \quad (\text{C.15})$$

where $\left. \frac{\partial \hat{Z}^{(1)}}{\partial \eta} \right|_{x_f^{(0)},\eta_j}$ can be obtained analytically from (5.32). Further,

$$\begin{aligned} T_{l,j+1}^{(1)} &= T_{x_{f-}^{(0)},j+1}^{(1)} + (x_l - x_f^{(0)}) \left. \frac{\partial T^{(1)}}{\partial x} \right|_{x_{f-}^{(0)},j+1} + \dots \\ &\dots + \frac{(x_l - x_f^{(0)})^2}{2} \left. \frac{\partial^2 T^{(1)}}{\partial x^2} \right|_{x_{f-}^{(0)},j+1} + \mathcal{O}(\Delta x^3) \text{ for } l = I, I-1. \end{aligned} \quad (\text{C.16})$$

Expanding $T_{I,j+1}^{(1)}$, $T_{I,j}^{(1)}$ using a Taylor expansion about $T_{I,j+\frac{1}{2}}^{(1)}$,

$$T_{I,j+1}^{(1)} = T_{x_{f-}^{(0)},j+\frac{1}{2}}^{(1)} + \frac{\Delta\eta}{2} \frac{\partial T^{(1)}}{\partial \eta} \Big|_{x_{f-}^{(0)},j+\frac{1}{2}} + \frac{1}{2} \left(\frac{\Delta\eta}{2} \right)^2 \frac{\partial^2 T^{(1)}}{\partial \eta^2} \Big|_{x_{f-}^{(0)},j+\frac{1}{2}} + \mathcal{O}(\Delta\eta^3), \quad (\text{C.17})$$

$$T_{I,j}^{(1)} = T_{x_{f-}^{(0)},j+\frac{1}{2}}^{(1)} - \frac{\Delta\eta}{2} \frac{\partial T^{(1)}}{\partial \eta} \Big|_{x_{f-}^{(0)},j+\frac{1}{2}} + \frac{1}{2} \left(\frac{\Delta\eta}{2} \right)^2 \frac{\partial^2 T^{(1)}}{\partial \eta^2} \Big|_{x_{f-}^{(0)},j+\frac{1}{2}} + \mathcal{O}(\Delta\eta^3). \quad (\text{C.18})$$

Substituting (C.8), (C.16)- (C.18) into (C.7), we have,

$$\begin{aligned} \tau = & \frac{\partial T^{(1)}}{\partial \eta} \Big|_{x_{f-}^{(0)},j+\frac{1}{2}} - \frac{1}{2} \left[(a_1^1 + a_2^1 + a_3^1) T_{x_{f-}^{(0)},j+1}^{(1)} + \{a_1^1(x_{I+1} - x_f^{(0)}) + \dots \right. \\ & \dots + a_2^1(x_I - x_f^{(0)}) + a_3^1(x_{I-1} - x_f^{(0)}) \} \frac{\partial T^{(1)}}{\partial x} \Big|_{x_{f-}^{(0)},j+1} + \dots \\ & \dots + \left\{ a_1^1 \frac{(x_{I+1} - x_f^{(0)})^2}{2} + a_2^1 \frac{(x_I - x_f^{(0)})^2}{2} + \dots \right. \\ & \dots + a_3^1 \frac{(x_{I-1} - x_f^{(0)})^2}{2} \} \frac{\partial^2 T^{(1)}}{\partial x^2} \Big|_{x_{f-}^{(0)},j+1} - C_{I,j+1} + \eta_{j+1}^2 \frac{dT^0}{dx} \Big|_{x_{f-}^{(0)}} + \dots \\ & \dots + \mathcal{O}(\Delta x) + a_1^1 \left\{ \llbracket T^{(1)} \rrbracket_{x_{f-}^{(0)},j+1} + (x_{I+1} - x_f^{(0)}) \llbracket \frac{\partial T^{(1)}}{\partial x} \rrbracket_{x_{f-}^{(0)},j+1} + \dots \right. \\ & \left. \dots + \frac{(x_{I+1} - x_f^{(0)})^2}{2} \llbracket \frac{\partial^2 T^{(1)}}{\partial x^2} \rrbracket_{x_{f-}^{(0)},j+1} \right\} + \Gamma \Big], \end{aligned} \quad (\text{C.19})$$

where,

$$\begin{aligned}
\Gamma = \frac{1}{2} & \left[(a_1 + a_2 + a_3) T_{x_{f^-,j}^{(0)}}^{(1)} + \{a_1(x_{I+1} - x_f^{(0)}) + a_2(x_I - x_f^{(0)}) + \dots \right. \\
& \dots + a_3(x_{I-1} - x_f^{(0)}) \} \frac{\partial T^{(1)}}{\partial x} \Big|_{x_{f^-,j}^{(0)}} + \left\{ a_1 \frac{(x_{I+1} - x_f^{(0)})^2}{2} + \dots \right. \\
& \dots + a_2 \frac{(x_I - x_f^{(0)})^2}{2} + a_3 \frac{(x_{I-1} - x_f^{(0)})^2}{2} \} \frac{\partial^2 T^{(1)}}{\partial x^2} \Big|_{x_{f^-,j}^{(0)}} + \dots \\
& \dots + a_1^1 \left\{ \llbracket T^{(1)} \rrbracket_{x_{f^-,j}^{(0)}} + (x_{I+1} - x_f^{(0)}) \llbracket \frac{\partial T^{(1)}}{\partial x} \rrbracket_{x_{f^-,j+1}^{(0)}} + \dots \right. \\
& \left. \dots + \frac{(x_{I+1} - x_f^{(0)})^2}{2} \llbracket \frac{\partial^2 T^{(1)}}{\partial x^2} \rrbracket_{x_{f^-,j}^{(0)}} \right\} - C_{I,j} + \eta_j^2 \frac{dT^0}{dx} \Big|_{x_{f^-}^{(0)}} + \mathcal{O}(\Delta x) \Big].
\end{aligned} \tag{C.20}$$

For making the truncation error, τ , in the equation (C.7) zero, we can bring the RHS of (C.19) to the form of (C.5) which is zero by making the imposing the following conditions,

$$a_1^1 + a_2^1 + a_3^1 = 0, \tag{C.21}$$

$$a_1^1(x_{I+1} - x_f^{(0)}) + a_2^1(x_I - x_f^{(0)}) + a_3^1(x_{I-1} - x_f^{(0)}) = \frac{2x_f^{(0)}}{\eta_j + \eta_{j+1}}, \tag{C.22}$$

$$a_1^1(x_{I+1} - x_f^{(0)})^2 + a_2^1(x_I - x_f^{(0)})^2 + a_3^1(x_{I-1} - x_f^{(0)})^2 = \frac{2}{\eta_j + \eta_{j+1}}, \tag{C.23}$$

$$\begin{aligned}
C_{I,j+1} = a_1^1 & \left(\llbracket T^{(1)} \rrbracket_{x_{f^-,j+1}^{(0)}} + (x_{I+1} - x_f^{(0)}) \llbracket \frac{\partial T^{(1)}}{\partial x} \rrbracket_{x_{f^-,j+1}^{(0)}} + \dots \right. \\
& \left. \dots + \frac{(x_{I+1} - x_f^{(0)})^2}{2} \llbracket \frac{\partial^2 T^{(1)}}{\partial x^2} \rrbracket_{x_{f^-,j+1}^{(0)}} \right).
\end{aligned} \tag{C.24}$$

Similar equations can be obtained for a_1 , a_2 , a_3 , $C_{I,j}$. Also, from (C.5) and (C.19), we can obtain,

$$\frac{f_{I,j+1} + f_{I,j}}{2} = - \frac{(\eta_{j+1}^2 + \eta_j^2) dT^0}{\eta_{j+1} + \eta_j dx} \Big|_{x_{f^-}^{(0)}}. \tag{C.25}$$

Similarly, we can write equation (C.5) at $x_{f+}^{(0)}$ as,

$$\begin{aligned}
\frac{\partial T^{(1)}}{\partial \eta} &= \frac{x_f^{(0)}}{\eta_j + \eta_{j+1}} \frac{\partial T^{(1)}}{\partial x} \Big|_{x_{f+}^{(0)},j} + \dots \\
\dots + \frac{x_f^{(0)}}{\eta_j + \eta_{j+1}} \frac{\partial T^{(1)}}{\partial x} \Big|_{x_{f+}^{(0)},j+1} &+ \frac{1}{2(\eta_j + \eta_{j+1})} \frac{\partial^2 T^{(1)}}{\partial x^2} \Big|_{x_{f+}^{(0)},j+1}, + \dots \quad (C.26) \\
\dots + \frac{1}{2(\eta_j + \eta_{j+1})} \frac{\partial^2 T^{(1)}}{\partial x^2} \Big|_{x_f^{(0)}-,j} &+ \frac{(\eta_{j+1}^2 + \eta_j^2)}{\eta_{j+1} + \eta_j} \frac{dT^0}{dx} \Big|_{x_{f+}^{(0)}}.
\end{aligned}$$

Further, we can write,

$$\begin{aligned}
\frac{T_{I+1,j+1}^{(1)} - T_{I+1,j}^{(1)}}{\Delta \eta} &= \frac{1}{2} \left\{ b_1^1 T_{I+2,j+1}^{(1)} + b_2^1 T_{I+1,j+1}^{(1)} + b_3^1 T_{I,j+1}^{(1)} + \dots \right. \\
\dots + b_1 T_{I+2,j}^{(1)} + b_2 T_{I+1,j}^{(1)} + b_3 T_{I,j}^{(1)} &- f_{I+1,j+1} - f_{I+1,j} - C_{I+1,j} - C_{I+1,j+1} \left. \right\}. \quad (C.27)
\end{aligned}$$

Using a similar methodology as was done for $x = x_I$, we obtain the following set of equations,

$$b_1^1 + b_2^1 + b_3^1 = 0, \quad (C.28)$$

$$b_1^1(x_{I+2} - x_f^{(0)}) + b_2^1(x_{I+1} - x_f^{(0)}) + b_3^1(x_I - x_f^{(0)}) = \frac{2x_f^{(0)}}{\eta_j + \eta_{j+1}}, \quad (C.29)$$

$$b_1^1(x_{I+2} - x_f^{(0)})^2 + b_2^1(x_{I+1} - x_f^{(0)})^2 + b_3^1(x_I - x_f^{(0)})^2 = \frac{2}{\eta_j + \eta_{j+1}}. \quad (C.30)$$

Further,

$$\begin{aligned}
C_{I+1,j+1} &= -b_3^1 \left\{ \llbracket T^{(1)} \rrbracket_{x_f^{(0)},j+1} + (x_{I+1} - x_f^{(0)}) \left[\left[\frac{\partial T^{(1)}}{\partial x} \right] \right]_{x_f^{(0)},j+1} + \dots \right. \\
&\quad \left. \dots + \frac{(x_{I+1} - x_f^{(0)})^2}{2} \left[\left[\frac{\partial^2 T^{(1)}}{\partial x^2} \right] \right]_{x_f^{(0)},j+1} \right\}, \quad (C.31)
\end{aligned}$$

$$\frac{f_{I+1,j+1} + f_{I+1,j}}{2} = - \frac{(\eta_{i+1}^2 + \eta_i^2)}{\eta_{i+1} + \eta_i} \frac{dT^0}{dx} \Big|_{x_{f+}^{(0)}}. \quad (C.32)$$

Similar equations can be obtained for b_1^1 , b_2^1 , b_3^1 , $C_{I+1,j}$.

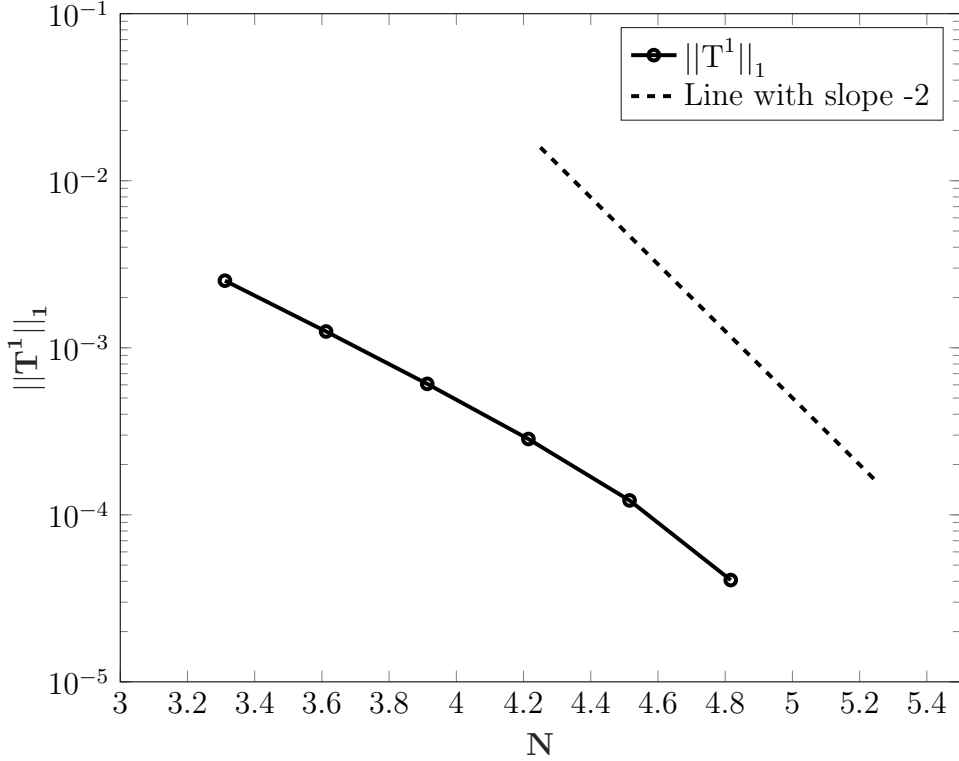


Figure C.2: Results of Grid Dependency studies on $T^{(1)}$ in terms of the L^1 norm, $\|T^{(1)}\|_1$ for $\mathcal{L}_F = 1.5$, $\mathcal{L}_O = 0.5$ and $\phi = 1$ as a function of the number of grid points, N

Once equation (6.4) has been discretized at all the points, the equations obtained are solved for $T^{(1)}$. Before the results, the scheme employed is validated with the help of a grid dependency test for which the L^1 norm of the error, $\|T^{(1)}\|_1$, defined as

$$\|T^{(1)}\|_1 = \sum_{i=1}^{N_0} \sum_{j=1}^{N_0} |T_{ref}^{(1)}(x_i, \eta_j) - T_N^{(1)}(x_i, \eta_j)| \Delta\eta \Delta x,$$

is plotted as shown in figure (C.2). Here, N_0 is the number of grid points in both the x and η directions corresponding to the test case $T_N^{(1)}$ is used. $T_{ref}^{(1)}$ corresponds to analytical solution obtained in equation (6.30) to compute the error. The results are shown in figure (C.2).